Mathematics

https://www.aimspress.com/journal/Math

AIMS Mathematics, 11(8): 25229–25264.
DOI: 10.3934/math.20261014
Received: 22 January 2026
Revised: 31 March 2026
Accepted: 14 April 2026
Published: 14 August 2026

Research article

A perturbed convex combination method for pseudo-monotone variational inequalities with applications to blood supply chain networks

Ghaziyah Alsahli[1,*], **Sani Salisu**[2,3] **and Nura Alotaibi**[1]

[1] Department of Mathematics, College of Sciences, Jouf University, Sakaka, P.O. Box 2014, Saudi Arabia

[2] School of Mathematical Sciences, Chongqing Normal University, Chongqing 401331, China

[3] Department of Mathematics, Faculty of Natural and Applied Sciences, Sule Lamido University, Kafin Hausa, Jigawa, Nigeria

* **Correspondence:** Email: gmsahli@ju.edu.sa; Tel: +966555981516.

Abstract: The paper proposes a new adaptive algorithm for solving variational inequality problems (VIPs) with pseudo-monotone operators. Such problems are central to modeling equilibrium in supply chain networks, where asymmetric cost structures lead to pseudo-monotonicity. The proposed method integrates convex combination techniques with an adaptive step-size criterion, requiring only a single metric projection per iteration. We prove linear convergence under strong pseudo-monotonicity and weak convergence under pseudo-monotonicity. Numerical experiments on a blood supply chain network with 24 routes and three demand scenarios show that the algorithm performs competitively with recent methods in terms of residual reduction and achieves the lowest execution time. The results demonstrate the algorithm's efficiency and scalability for large-scale network optimization, with potential impact on healthcare logistics and related applications.

Keywords: variational inequality; adaptive algorithm; supply chain network; pseudo-monotone; convex combination; linear convergence rate
Mathematics Subject Classification: 47H05, 49J40, 49M37, 90B50, 90C25, 90C30

1. Introduction

For $\mathcal{H}$, a real Hilbert space with a nonempty subset $C \subset \mathcal{H}$ and a mapping $\mathcal{A} : \mathcal{H} \to \mathcal{H}$, we consider the problem

$$\text{find } w^* \in C \text{ such that } \langle \mathcal{A}(w^*), w - w^* \rangle \geq 0, \quad \forall w \in C. \tag{1.1}$$

This problem is referred to as a *variational inequality problem* (VIP). Variational inequalities naturally arise as first-order optimality conditions for constrained optimization problems involving differentiable convex functions. The systematic study of problems of the form (1.1) dates back to the work of Lions and Stampacchia [1] in finite-dimensional spaces and was later considered in infinite-dimensional settings; see, for instance, [2, 3] and the references therein. Owing to their generality, variational inequality formulations have found extensive applications across science, economics, and engineering [4–6].

VIPs constitute a powerful and unifying framework that encompasses a broad class of equilibrium and optimization models arising in practice. Applications of VIPs include economic equilibrium and game-theoretic models [7, 8]; contact and friction problems in engineering mechanics [9, 10]; constrained optimization and saddle-point formulations in mathematical programming [11, 12]; traffic flow and network equilibrium problems in transportation science [13]; as well as models from applied sciences such as structural analysis and fluid dynamics [14]. As a consequence of this wide applicability, variational inequalities play a central role in modern mathematical analysis, bridging theoretical developments with real-world modeling.

A classical approach to solving VIPs relies on fixed point schemes obtained through the use of the metric projection $\Pi_C : \mathcal{H} \to C$ onto a closed and convex set C. This projection operator is characterized by the inequality

$$\langle w - \Pi_C(w),\, z - \Pi_C(w)\rangle \leq 0, \quad \forall\, z \in C,\ \forall\, w \in \mathcal{H}. \tag{1.2}$$

This characterization ensures that a point $w^* \in C$ is a solution of (1.1) if and only if it satisfies the fixed point equation

$$w^* = \Pi_C(w^* - \beta\mathcal{A}(w^*)), \tag{1.3}$$

where $\beta > 0$. As a consequence of this equivalence, several projection-type fixed point iterations have been developed for solving VIPs. A substantial example is the Picard iteration

$$w_{n+1} = \Pi_C(w_n - \beta\mathcal{A}(w_n)),$$

commonly known as the *projected gradient method*.

This method is guaranteed to converge provided that the operator $\mathcal{A}$ is either strongly monotone or inverse strongly monotone, together with a suitable choice of the step-size parameter β; see, for instance, [15–17]. However, these assumptions are often restrictive. To relax the assumptions, Korpelevich [18] introduced the celebrated *extragradient method*, defined by the iterative scheme

$$\begin{cases} u_n = \Pi_C(w_n - \beta\mathcal{A}(w_n)), \\ w_{n+1} = \Pi_C(w_n - \beta\mathcal{A}(u_n)). \end{cases} \tag{1.4}$$

This method converges for monotone and Lipschitz continuous operators and therefore significantly enlarges the class of solvable VIPs. Compared to the projected gradient method, extragradient relaxes the strong monotonicity requirement to just monotone. However, each iteration requires two metric projections and two evaluations of the operator $\mathcal{A}$, which may increase the computational cost in large-scale settings.

Since the introduction of the extragradient method (1.4), numerous refinements have been proposed with the aim of reducing computational cost while preserving convergence guarantees. For example, Popov's extragradient method [19] decreases the number of operator evaluations by efficiently reusing information from previous iterations. The subgradient extragradient method [20, 21] replaces the second projection onto the feasible set C with a projection onto a suitably constructed half-space, which often admits a closed-form expression and is therefore particularly attractive for large-scale problems.

Projection and contraction methods [22] incorporate an additional contraction step to enhance convergence speed, especially when strong monotonicity is present. Other developments based on reflected–gradient ideas include the projected reflected–gradient algorithm [23] and the forward–reflected–backward algorithm [24]. Moreover, step-size strategies motivated by geometric considerations have led to the golden ratio algorithm [25].

The subgradient extragradient method [20] and other extragradient variants [26, 27] have further enriched the field. Dual extrapolation techniques [28] and modified forward-backward splitting [29] provide alternative perspectives. Recent contributions include modified projected gradient methods [30], effective iterative projection schemes [31], and inertial contraction approaches [32]. Fully adaptive methods for quasi–monotone problems [33] and hierarchical variational inequalities on manifolds [34] represent further progress. Unified schemes for split inclusions [35], Halpern-type mean subgradient extragradient methods [36], and accelerated hybrid Mann-type algorithms [37] have also been studied. Additional approximation techniques for monotone inclusions and variational inequalities can be found in [38–40], while extragradient methods in CAT(0) spaces [41] extend the theory to non-Euclidean geometries. Collectively, these contributions highlight the flexibility of projection-based methods and their continuous evolution in response to increasing computational demands.

Most of the recent developments include the use of adaptive step-size rules that do not require knowledge of the Lipschitz constant [33], and the incorporation of viscosity terms to achieve strong convergence [34]. In particular, methods based on the golden ratio [25] have shown remarkable acceleration for monotone operators, while inertial techniques have been extended to pseudo-monotone settings [42, 53].

Among projection-based algorithms, the forward–backward–forward method, commonly referred to as Tseng's algorithm [29], has emerged as an efficient alternative to the classical extragradient scheme. This method is defined by the iterative process

$$\begin{cases} u_n = \Pi_C(w_n - \beta_n \mathcal{A}(w_n)), \\ w_{n+1} = u_n - \beta_n(\mathcal{A}(u_n) - \mathcal{A}(w_n)), \end{cases} \tag{1.5}$$

and requires only one projection per iteration. By incorporating an explicit correction step involving differences of the operator, it significantly reduces computational complexity while maintaining convergence under less restrictive conditions. Tseng's forward–backward–forward method reduces the projection cost to one per iteration while retaining convergence under monotonicity, making it more suitable for large-scale problems. Owing to its close connection with forward–backward splitting, this algorithm is particularly well suited for large-scale and stochastic settings, where per-iteration efficiency is critical.

To further enhance convergence performance, inertial or momentum-based extrapolation techniques have been integrated into such schemes, drawing inspiration from acceleration principles such as Nesterov's method and the heavy-ball approach. Inertial variants of the forward–backward–forward algorithm introduce momentum terms that exploit information from previous iterates, often resulting in faster convergence and improved numerical stability, especially for ill-conditioned or nonsmooth problems. Weak convergence results for these inertial schemes have been established [42, 43]; linear convergence rates under appropriate assumptions are derived in [44, 45]; and successful applications to a variety of practical models are reported in [46–48]. Further developments include modified Tseng-type methods [49], accelerated forward-backward-half-forward splitting [50], and inertial Tseng methods for image recovery [51]. Collectively, these contributions demonstrate the effectiveness of single-inertial strategies.

Recently, double inertial extrapolation strategies have been introduced, in which two distinct momentum terms are incorporated into the iterative process. An example is the double inertial forward–backward–forward algorithm investigated in [50]. By combining multiple extrapolated points within the update rule, such schemes aim to further amplify acceleration effects beyond those achieved by single-inertial methods. Under suitable choices of parameters, double inertial algorithms have demonstrated improved convergence properties and enhanced numerical performance, which has stimulated growing interest in their theoretical analysis and practical applications; see, for instance, [52, 53] (viscosity and relaxed Tseng methods) and [54, 55] (single-projection and self-adaptive strategies). These inertial variants accelerate convergence in practice, but they typically require two projections or involve more complex parameter tuning.

The development of variational inequality algorithms is largely motivated by their ability to approximate solutions to models arising from a wide range of real-world phenomena. In particular, the optimization of supply chain networks has become a critical concern in today's competitive and resource-constrained environment, where organizations must innovate while minimizing costs in the face of increasing demand and persistent economic challenges. Supply chains involving perishable goods, such as food, pharmaceuticals, and blood, are especially complex due to limited shelf life and the high disposal costs associated with excess inventory [56–58].

Effective mathematical models are therefore essential for addressing issues related to preservation time, surplus management, and the resulting financial and operational implications. Blood supply chains, encompassing collection, processing, storage, and distribution, pose additional challenges, including shortages that disrupt medical services and oversupply that leads to waste and environmental concerns [56, 59]. These challenges necessitate models that explicitly account for perishability, processing losses, capacity constraints, and uncertain hospital demand.

Recent advances in supply chain modeling from various methodological perspectives can be found in [60–68] and the references therein. Within this context, Semenov and Denysov [59] proposed a computational framework for comparing several adaptive variants of extragradient-type methods. Their study examined the numerical behavior of these algorithms on a blood supply chain network using a software platform that allows flexible adjustment of model parameters. A key feature of these adaptive schemes is that they do not require prior knowledge of the Lipschitz constant of the underlying operator, while still preserving convergence and computational efficiency. The three adaptive algorithms considered in [59], which may be viewed as adaptive counterparts of Popov's method, Tseng's method, and a forward–reflected gradient scheme, update the step size dynamically using only information generated during the iterative process.

Following this line of research, a perturbed variant of Tseng's forward–backward–forward algorithm was introduced in [69] for the effective solution of blood supply chain network problems.

Starting from an initial point $w_0 \in \mathcal{H}$, with $\beta_0 > 0$, $\lambda \in (0, 1)$, and $d_0 = -\mathcal{A}(w_0)$, the method generates sequences $\{w_n\}$, $\{z_n\}$, and $\{d_n\}$ iteratively based on

$$\begin{cases} z_n = \Pi_C(w_n + \beta_n d_n)\,, \\ w_{n+1} = z_n + \beta_n(\mathcal{A}(w_n) - \mathcal{A}(z_n)), \\ d_{n+1} = -\mathcal{A}(w_{n+1}) + \xi_n d_n, \\ \beta_{n+1} = \min\left\{\beta_n,\ \dfrac{\sigma\|w_n - z_n\|}{\|\mathcal{A}(w_n) - \mathcal{A}(z_n)\|}\right\}. \end{cases} \tag{1.6}$$

The numerical experiments reported therein illustrate the effectiveness of the proposed scheme on a realistic blood supply network comprising of collection sites, processing and storage facilities, distribution centers, and demand points. The results underscore the broad applicability of the algorithm within real Hilbert spaces, highlighting its potential for addressing a wide class of optimization problems and for supporting improved decision-making and operational efficiency in blood supply chains and related application domains.

To provide a clear overview of key developments, Table 1 summarizes the some of the methods, highlighting the operator type, per-iteration operator evaluations and projections, and step-size strategy.

Table 1. Comparison of selected popular variational inequality algorithms.

Method	Operator type	Operator evaluations per iteration	Projections per iteration	Step-size
Projected gradient [15, 16]	strongly monotone	1	1	fixed
Extragradient [18]	monotone	2	2	fixed
Popov's extragradient [19]	monotone	1	2	fixed
Subgradient extragradient [20, 21]	monotone	2	1	fixed/adaptive
Tseng's forward–backward–forward [29]	monotone	2	1	adaptive
Golden ratio algorithm [25]	monotone	2	1	fixed
Forward–reflected–backward [24]	monotone	2	1	adaptive
Double inertial Tseng [50]	monotone	2	1	adaptive
Single projection with double inertial [54]	pseudo-monotone	2	1	adaptive

The aim of this work is to propose an efficient method for approximating solutions of VIPs, with specific applications such as blood supply chain networks. To this end, we introduce a new algorithm based on convex combination techniques, which approximates solutions even when the underlying operator is pseudo-monotone rather than monotone. The algorithm requires only a single computation of the metric projection per iteration and incorporates an adaptive step-size criterion. Table 1 situates the proposed algorithm within the current literature.

A key contribution of the proposed method lies in its combination of convex combination ideas with an adaptive step-size rule, enabling it to handle pseudo-monotone operators while retaining strong theoretical and geometrical properties. We establish that the generated sequence converges to a solution of the variational inequality and further prove linear convergence under strong pseudo-monotonicity. In addition, the requirement of only one metric projection per iteration enhances computational efficiency, making the method well suited for large-scale applications. To demonstrate its practical relevance, we provide a numerical illustration on a blood supply chain network, comparing the method with state-of-the-art algorithms and showing its competitiveness and reliability. Moreover, we illustrate how the method can be applied to support efficient blood supply management, in line with recent studies [59, 69]. This is particularly important, as blood supply chain management is critical to healthcare systems and requires reliable strategies to meet fluctuating demand. Finally, we present a generic non-monotone (but pseudo-monotone) example, demonstrating the method's strong performance relative to recently developed algorithms.

2. Preliminaries

Let $\mathcal{H}$ be a real Hilbert space equipped with the inner product $\langle \cdot, \cdot \rangle$ and the induced norm $\|\cdot\|$. Recall that in such spaces, for any $w, y \in \mathcal{H}$, the polarization identity holds:

$$2\langle w, y\rangle = \|w\|^2 + \|y\|^2 - \|w - y\|^2 = \|w + y\|^2 - \|w\|^2 - \|y\|^2,$$

and, equivalently, we have

$$\|w - y\|^2 + \|w + y\|^2 = 2\|w\|^2 + 2\|y\|^2.$$

These elementary relations play a crucial role in deriving energy-type estimates and error bounds for the iterative schemes studied later.

Throughout the paper, we consider an operator $\mathcal{A} : \mathcal{H} \to \mathcal{H}$ endowed with standard regularity properties commonly used in variational inequality theory. In particular, $\mathcal{A}$ is said to be monotone on $\mathcal{H}$ if

$$\langle \mathcal{A}(w) - \mathcal{A}(y),\ w - y\rangle \geq 0, \qquad \forall\, w, y \in \mathcal{H}.$$

Moreover, $\mathcal{A}$ is called η-strongly pseudo-monotone, for some $\eta > 0$, if for all $w, y \in \mathcal{H}$, the implication

$$\langle \mathcal{A}(y),\ w - y\rangle \geq 0 \quad \Longrightarrow \quad \langle \mathcal{A}(w),\ w - y\rangle \geq \eta\|w - y\|^2$$

holds. The operator $\mathcal{A}$ is said to be pseudo-monotone if

$$\langle \mathcal{A}(w),\ y - w\rangle \geq 0 \quad \Longrightarrow \quad \langle \mathcal{A}(y),\ y - w\rangle \geq 0, \qquad \forall\, w, y \in \mathcal{H},$$

and it is called L-Lipschitz continuous on $\mathcal{H}$ if there exists a constant $L > 0$ such that

$$\|\mathcal{A}(w) - \mathcal{A}(y)\| \leq L\|w - y\|, \qquad \forall\, w, y \in \mathcal{H}.$$

Besides the generic situation illustrated in Example 5.1, pseudo-monotone operators arise naturally in a wide range of equilibrium problems where classical monotonicity assumptions are too restrictive. For example, in traffic assignment models, travel cost functions are often asymmetric due to congestion and network effects, leading to formulations that are not monotone but still pseudo-monotone. Similarly, economic equilibrium models with non-symmetric or nonlinear cost structures, as well as supply chain and network flow problems with congestion effects, frequently give rise to pseudo-monotone variational inequalities [70, 71]. Furthermore, pseudo-monotonicity provides a flexible framework that captures these real-world features while ensuring the existence of equilibria under suitable conditions and allowing the development of convergent numerical methods. Therefore, the study of VIPs involving pseudo-monotone operators is both theoretically significant and practically relevant.

Let $C \subset \mathcal{H}$ be a nonempty, closed, and convex set. For any $w \in \mathcal{H}$, there exists a unique point $\Pi_C(w) \in C$, called the metric projection of w onto C (see, e.g., [72]). This projection operator enjoys several fundamental properties that will be repeatedly used in the analysis. In particular, it is firmly non-expansive in the sense that for all $w, y \in \mathcal{H}$,

$$\langle w - y,\ \Pi_C(w) - \Pi_C(y)\rangle \geq \|\Pi_C(w) - \Pi_C(y)\|^2, \tag{2.1}$$

which guarantees that

$$\|w - z\|^2 \geq \|w - \Pi_C(w)\|^2 + \|z - \Pi_C(z)\|^2, \quad \forall\, w \in \mathcal{H},\ \forall\, z \in C. \tag{2.2}$$

Lemma 2.1. *[73] Let $\{w_n\} \subset \mathcal{H}$ and $\mathcal{D} \subset \mathcal{H}$ satisfy:*

(i) $\lim_{n\to\infty} \|w_n - w_*\|$ *exists for every $w_* \in \mathcal{D}$;*

(ii) Every weak cluster point of $\{w_n\}$ belongs to $\mathcal{D}$.

Then $\{w_n\}$ converges weakly to some $w^* \in \mathcal{D}$.

Lemma 2.2. *[74] Let $\mathcal{A} : C \to \mathcal{H}$ be pseudo-monotone and continuous. Then, the following are equivalent for $\hat{w} \in C$:*

(i) $\hat{w}$ solves the VIP (1.1)*;*

(ii) $\langle \mathcal{A}(w), w - \hat{w}\rangle \geq 0,\ \ w \in C$.

With the necessary notation and preliminary results established, we now introduce the proposed perturbed convex combination algorithm.

3. Perturbed convex combination algorithm and its convergence analysis

This section presents a perturbed convex combination algorithm with a step size supporting adaptive strategies for solving VIPs involving pseudo-monotone mappings in the framework of real Hilbert spaces. The section also discusses the convergence analysis of the sequence generated by the algorithm.

Remark 3.1. Algorithm 1 is well-defined considering that there are many possible choices of step sizes that satisfy the required condition. For instance, one could consider the following update:

(S1) For the given σ and β_n, define $\beta_{n+1} := \min\left\{\beta_n,\ \sigma\dfrac{\|w_n - z_n\|}{\|\mathcal{A}(w_n) - \mathcal{A}(z_n)\|}\right\}$.

(S2) For any $\tau \in [0, 1]$, define $\beta_{n+1} := \dfrac{\tau\sigma}{L}$.

Selecting any of the two forms above as the step size, one can easily establish the required condition

$$\beta_{n+1}\|\mathcal{A}(w_n) - \mathcal{A}(z_n)\| \leq \sigma\|w_n - z_n\|.$$

Moreover, the two selections provide a sequence of iterates of step lengths that converges to a positive real number. Note that this convergence property for the second step size is trivial, while for the first case, you can note that $\beta_{n+1} \leq \beta_n$ for all $n > 1$, and the Lipschitz condition on $\mathcal{A}$ guarantees that

$$\beta_{n+1} \geq \min\left\{\beta_n, \lambda\frac{\|w_n - z_n\|}{\|\mathcal{A}(w_n) - \mathcal{A}(z_n)\|}\right\} \geq \min\left\{\beta_n, \frac{\lambda}{L}\right\}.$$

Thus, by induction, we get that $\beta_n \geq \min\left\{\beta_1, \dfrac{\lambda}{L}\right\}$ for all $n > 1$, which implies that $\{\beta_n\}$ is a monotonic decreasing sequence that is bounded below, and thus, converges to its infimum.

Algorithm 1 Perturbed Convex Combination Algorithm with Adaptive Step Size

1: Select $\beta_1 > 0, \chi \in \left(0, \frac{1}{2}\right), \sigma \in \left(0, \frac{1}{\sqrt{2}}\right)$, and initial points $z_0, z_1 \in \mathcal{H}$.

2: Set $w_1 = \Pi_C\left(\chi z_0 + (1-\chi)z_1 - \beta_1\mathcal{A}(z_1)\right)$.

3: Having z_n and w_n, compute

$$z_{n+1} = w_n + \beta_n(\mathcal{A}(z_n) - \mathcal{A}(w_n)).$$

4: Update β_{n+1} such that

$$\beta_{n+1}\|\mathcal{A}(w_n) - \mathcal{A}(z_n)\| \leq \sigma\|w_n - z_n\|. \tag{3.1}$$

5: Compute the next iterate

$$w_{n+1} = \Pi_C\left(\chi z_n + (1-\chi)z_{n+1} - \beta_{n+1}\mathcal{A}(z_{n+1})\right).$$

6: Update $n \leftarrow n + 1$ and return to step 3.

Theorem 3.2. *Suppose that $\mathcal{A} : \mathcal{H} \to \mathcal{H}$ is a pseudo-monotone mapping, and that $\mathcal{S} \neq \emptyset$. Let $\{w_n\}$ and $\{z_n\}$ be sequences generated by Algorithm 1. For any $x^* \in \mathcal{S}$, define the sequence*

$$a_n := \|z_n - x^*\|^2 + \chi\|z_{n-1} - x^*\|^2.$$

Then, the following inequality holds:

$$a_{n+1} \quad \leq \quad a_n + \chi(2\chi - 1)\|z_n - z_{n-1}\|^2 - \left(\frac{1}{2} - \frac{\beta_n^2}{\beta_{n+1}^2}\sigma^2\right)\|w_n - z_n\|^2. \tag{3.2}$$

Furthermore, if the sequence $\{\beta_n/\beta_{n+1}\}$ converges to a number less than or equal to 1, then the sequence $\{a_n\}$ converges as well, and consequently,

$$\lim_{n\to\infty}\|z_n - z_{n-1}\| = 0 \quad \textit{and} \quad \lim_{n\to\infty}\|w_n - z_n\| = 0.$$

Proof. Take $x^* \in \mathcal{S}$. Then

$$\langle\mathcal{A}(x^*), y - x^*\rangle \geq 0, \quad \forall y \in C,$$

which implies that $\langle \mathcal{A}(x^*), w_n - x^* \rangle \geq 0$ since $w_n \in C$. Consequently, $\mathcal{A}$ being pseudo-monotone yields

$$\langle \mathcal{A}(w_n), w_n - x^* \rangle \geq 0. \tag{3.3}$$

Now, from

$$w_n = \Pi_C((\chi z_{n-1} + (1-\chi)z_n) - \beta_n \mathcal{A}(z_n)),$$

we get

$$\langle w_n - (\chi z_{n-1} + (1-\chi)z_n) + \beta_n \mathcal{A}(z_n), x^* - w_n \rangle \geq 0. \tag{3.4}$$

Hence, from (3.3), we obtain

$$\langle \beta_n \mathcal{A}(w_n), w_n - x^* \rangle \geq 0 \Leftrightarrow \langle -\beta_n \mathcal{A}(w_n), x^* - w_n \rangle \geq 0.$$

Add this inequality to (3.4), and we obtain

$$\langle w_n - (\chi z_{n-1} + (1-\chi)z_n) + \beta_n \mathcal{A}(z_n) - \beta_n \mathcal{A}(w_n), x^* - w_n \rangle \geq 0. \tag{3.5}$$

We have from $z_{n+1} = w_n + \beta_n(\mathcal{A}(z_n) - \mathcal{A}(w_n))$ and (3.5) that

$$\langle z_{n+1} - (\chi z_{n-1} + (1-\chi)z_n), x^* - w_n \rangle \geq 0. \tag{3.6}$$

Consequently, we have from (3.6) that

$$\begin{aligned} 0 &\leq \langle z_{n+1} - (\chi z_{n-1} + (1-\chi)z_n), x^* - w_n \rangle \\ &= \langle z_{n+1} - (\chi z_{n-1} + (1-\chi)z_n), x^* - z_{n+1} + z_{n+1} - w_n \rangle \\ &= \langle z_{n+1} - (\chi z_{n-1} + (1-\chi)z_n), x^* - z_{n+1} \rangle \\ &\quad + \langle z_{n+1} - (\chi z_{n-1} + (1-\chi)z_n), z_{n+1} - w_n \rangle. \end{aligned}$$

So, we get

$$\begin{aligned} &\langle z_{n+1} - (\chi z_{n-1} + (1-\chi)z_n), z_{n+1} - x^* \rangle \\ \leq\ & \langle z_{n+1} - (\chi z_{n-1} + (1-\chi)z_n), z_{n+1} - w_n \rangle \\ =\ & \langle z_{n+1} - (\chi z_{n-1} + (1-\chi)z_n), z_{n+1} - (\chi z_{n-1} + (1-\chi)z_n) \rangle \\ & + \langle z_{n+1} - (\chi z_{n-1} + (1-\chi)z_n), \chi z_{n-1} + (1-\chi)z_n - w_n \rangle \\ =\ & \|z_{n+1} - (\chi z_{n-1} + (1-\chi)z_n)\|^2 \\ & + \langle z_{n+1} - (\chi z_{n-1} + (1-\chi)z_n), \chi z_{n-1} + (1-\chi)z_n - w_n \rangle \\ =\ & \|z_{n+1} - (\chi z_{n-1} + (1-\chi)z_n)\|^2 \\ & + \langle \chi z_{n-1} + (1-\chi)z_n - w_n, w_n + \beta_n(\mathcal{A}(z_n) - \mathcal{A}(w_n)) - (\chi z_{n-1} + (1-\chi)z_n) \rangle \\ =\ & \|z_{n+1} - (\chi z_{n-1} + (1-\chi)z_n)\|^2 - \|w_n - (\chi z_{n-1} + (1-\chi)z_n)\|^2 \\ & + \beta_n \langle \chi z_{n-1} + (1-\chi)z_n - w_n, \mathcal{A}(z_n) - \mathcal{A}(w_n) \rangle. \end{aligned} \tag{3.7}$$

Also,

$$2\langle z_{n+1} - (\chi z_{n-1} + (1-\chi)z_n), z_{n+1} - x^* \rangle$$

$$
\begin{aligned}
&= \|\chi z_{n-1} + (1-\chi)z_n - z_{n+1}\|^2 - \|\chi z_{n-1} + (1-\chi)z_n - x^*\|^2 \\
&\quad + \|z_{n+1} - x^*\|^2.
\end{aligned} \tag{3.8}
$$

If we plug (3.8) into (3.7), we get

$$
\begin{aligned}
& \|\chi z_{n-1} + (1-\chi)z_n - z_{n+1}\|^2 - \|\chi z_{n-1} + (1-\chi)z_n - x^*\|^2 + \|z_{n+1} - x^*\|^2 \\
\leq\ & 2\|z_{n+1} - (\chi z_{n-1} + (1-\chi)z_n)\|^2 - 2\|w_n - (\chi z_{n-1} + (1-\chi)z_n)\|^2 \\
& +2\beta_n\langle \chi z_{n-1} + (1-\chi)z_n - w_n, \mathcal{A}(z_n) - \mathcal{A}(w_n)\rangle.
\end{aligned}
$$

Therefore,

$$
\begin{aligned}
\|z_{n+1} - x^*\|^2 \leq\ & \|\chi z_{n-1} + (1-\chi)z_n - x^*\|^2 + \|z_{n+1} - (\chi z_{n-1} + (1-\chi)z_n)\|^2 \\
& -2\|\chi z_{n-1} + (1-\chi)z_n - w_n\|^2 \\
& +2\beta_n\langle \chi z_{n-1} + (1-\chi)z_n - w_n, \mathcal{A}(z_n) - \mathcal{A}(w_n)\rangle.
\end{aligned} \tag{3.9}
$$

Now,

$$
\begin{aligned}
& \|z_{n+1} - (\chi z_{n-1} + (1-\chi)z_n)\|^2 \\
=\ & \|w_n - (\chi z_{n-1} + (1-\chi)z_n) + \beta_n\mathcal{A}(z_n) - \beta_n\mathcal{A}(w_n)\|^2 \\
=\ & \|w_n - (\chi z_{n-1} + (1-\chi)z_n)\|^2 + 2\beta_n\langle w_n - (\chi z_{n-1} + (1-\chi)z_n), \mathcal{A}(z_n) - \mathcal{A}(w_n)\rangle \\
& +\beta_n^2\|\mathcal{A}(z_n) - \mathcal{A}(w_n)\|^2.
\end{aligned} \tag{3.10}
$$

If we plug (3.10) into (3.9), we get

$$
\begin{aligned}
\|z_{n+1} - x^*\|^2 \leq\ & \|\chi z_{n-1} + (1-\chi)z_n - x^*\|^2 - \|\chi z_{n-1} + (1-\chi)z_n - w_n\|^2 \\
& +\beta_n^2\|\mathcal{A}(z_n) - \mathcal{A}(w_n)\|^2.
\end{aligned} \tag{3.11}
$$

Using the parallelogram identity, we get

$$
\begin{aligned}
& \|w_n - z_n\|^2 + \|(\chi z_{n-1} + (1-\chi)z_n - w_n) + (\chi z_{n-1} + (1-\chi)z_n - z_n)\|^2 \\
=\ & 2\|\chi z_{n-1} + (1-\chi)z_n - w_n\|^2 + 2\|\chi z_{n-1} + (1-\chi)z_n - z_n\|^2,
\end{aligned}
$$

and so

$$
\|\chi z_{n-1} + (1-\chi)z_n - w_n\|^2 \geq -\|\chi z_{n-1} + (1-\chi)z_n - z_n\|^2 + \frac{1}{2}\|w_n - z_n\|^2. \tag{3.12}
$$

Using (3.12) in (3.11), we obtain that

$$
\begin{aligned}
\|z_{n+1} - x^*\|^2 \leq\ & \|\chi z_{n-1} + (1-\chi)z_n - x^*\|^2 + \|\chi z_{n-1} + (1-\chi)z_n - z_n\|^2 \\
& -\frac{1}{2}\|w_n - z_n\|^2 + \beta_n^2\|\mathcal{A}(z_n) - \mathcal{A}(w_n)\|^2 \\
\leq\ & \|\chi z_{n-1} + (1-\chi)z_n - x^*\|^2 + \|\chi z_{n-1} + (1-\chi)z_n - z_n\|^2 \\
& -\frac{1}{2}\|w_n - z_n\|^2 + \frac{\beta_n^2}{\beta_{n+1}^2}\beta_{n+1}^2\|\mathcal{A}(z_n) - \mathcal{A}(w_n)\|^2
\end{aligned}
$$

$$
\begin{aligned}
&\leq \|\chi z_{n-1} + (1-\chi)z_n - x^*\|^2 + \|\chi z_{n-1} + (1-\chi)z_n - z_n\|^2 \\
&\quad -\frac{1}{2}\|w_n - z_n\|^2 + \frac{\beta_n^2}{\beta_{n+1}^2}\sigma^2\|z_n - w_n\|^2 \\
&= \|\chi z_{n-1} + (1-\chi)z_n - x^*\|^2 + \|\chi z_{n-1} + (1-\chi)z_n - z_n\|^2 \\
&\quad -\Big(\frac{1}{2} - \frac{\beta_n^2}{\beta_{n+1}^2}\sigma^2\Big)\|w_n - z_n\|^2. \qquad (3.13)
\end{aligned}
$$

Thus, we get

$$
\begin{aligned}
\|\chi z_{n-1} + (1-\chi)z_n - x^*\|^2 &= \chi\|z_{n-1} - x^*\|^2 + (1-\chi)\|z_n - x^*\|^2 \\
&\quad -\chi(1-\chi)\|z_n - z_{n-1}\|^2.
\end{aligned}
$$

Also,

$$
\|\chi z_{n-1} + (1-\chi)z_n - z_n\|^2 = \chi^2\|z_n - z_{n-1}\|^2.
$$

Hence,

$$
\begin{aligned}
\|\chi z_{n-1} + (1-\chi)z_n - x^*\|^2 + \|\chi z_{n-1} + (1-\chi)z_n - z_n\|^2 &= \chi\|z_{n-1} - x^*\|^2 + (1-\chi)\|z_n - x^*\|^2 \\
&\quad + \chi(2\chi - 1)\|z_n - z_{n-1}\|^2. \qquad (3.14)
\end{aligned}
$$

Plugging (3.14) into (3.13), we get

$$
\begin{aligned}
\|z_{n+1} - x^*\|^2 &\leq \chi\|z_{n-1} - x^*\|^2 + (1-\chi)\|z_n - x^*\|^2 \\
&\quad +\chi(2\chi - 1)\|z_n - z_{n-1}\|^2 - \Big(\frac{1}{2} - \frac{\beta_n^2}{\beta_{n+1}^2}\sigma^2\Big)\|w_n - z_n\|^2.
\end{aligned}
$$

Hence,

$$
\begin{aligned}
\|z_{n+1} - x^*\|^2 + \chi\|z_n - x^*\|^2 &\leq \|z_n - x^*\|^2 + \chi\|z_{n-1} - x^*\|^2 + \chi(2\chi - 1)\|z_n - z_{n-1}\|^2 \\
&\quad - \Big(\frac{1}{2} - \frac{\beta_n^2}{\beta_{n+1}^2}\sigma^2\Big)\|w_n - z_n\|^2. \qquad (3.15)
\end{aligned}
$$

We then have from (3.15) that

$$
a_{n+1} \leq a_n + \chi(2\chi - 1)\|z_n - z_{n-1}\|^2 - \Big(\frac{1}{2} - \frac{\beta_n^2}{\beta_{n+1}^2}\sigma^2\Big)\|w_n - z_n\|^2, \qquad (3.16)
$$

where $a_n := \|z_n - x^*\|^2 + \chi\|z_{n-1} - x^*\|^2$. Since $\chi(2\chi - 1) < 0$ and the sequence $\{\beta_n/\beta_{n+1}\}$ converges to a number less than or equal to 1, we conclude that the sequence $\{a_n\}$ is monotone nonincreasing and possesses a limit. Consequently, the desired results are achieved. □

Next, we provide a result with sufficient conditions to guarantee the convergence of the sequence generated by the proposed algorithm to an element of $\mathcal{S}$. To establish the convergence, the following condition is crucial. A mapping $\mathcal{A} : \mathcal{H} \to \mathcal{H}$ is said to satisfy Condition A if

$$
\left.\begin{aligned} w_n \rightharpoonup y \quad \text{and} \\ \liminf_{n\to\infty} \|\mathcal{A}(w_n)\| = 0 \end{aligned}\right\} \implies \mathcal{A}(y) = 0. \qquad (3.17)
$$

Remark 3.3. Condition A is satisfied by several important classes of operators commonly encountered in applications. In particular, continuous monotone operators, such as gradients of differentiable convex functions, satisfy this condition, thereby covering a broad range of optimization models. In finite-dimensional settings ($\mathcal{H} = \mathbb{R}^d$), continuous pseudo-monotone operators also satisfy Condition A. These classes arise frequently in practice, including in optimization, equilibrium, and variational models, making the assumption widely applicable. Moreover, Condition A is typically easy to verify in applications, as it follows directly from standard properties such as monotonicity, continuity, or convexity of the underlying problem. Since Condition A is a theoretical property and does not involve any parameter to be chosen by the user, it imposes no additional implementation burden.

Theorem 3.4. *Suppose that $\mathcal{A} : \mathcal{H} \to \mathcal{H}$ is an L-Lipschitz pseudo-monotone mapping that satisfies Condition A. Let $\mathcal{S} \neq \emptyset$ and suppose the sequence $\{\beta_n/\beta_{n+1}\}$ converges to a number less than or equal to 1. Then the sequences $\{z_n\}$ and $\{w_n\}$ generated by Algorithm 1 both converge weakly to an element of $\mathcal{S}$.*

Proof. By Theorem 3.2, we have that

$$\lim_{n\to\infty} \|z_{n-1} - z_n\| = 0 \quad \text{and} \quad \lim_{n\to\infty} \|z_n - w_n\| = 0.$$

Consequently,

$$\lim_{n\to\infty} \|\chi z_{n-1} + (1-\chi)z_n - z_n\| = 0,$$

and

$$\|w_n - (\chi z_{n-1} + (1-\chi)z_n)\| \leq \|w_n - z_n\| + \|\chi z_{n-1} + (1-\chi)z_n - z_n\| \to 0, \ n \to \infty.$$

By the fact assumption that $\mathcal{A}$ is Lipschitz continuous, we have

$$\lim_{n\to\infty} \|\mathcal{A}(z_n) - \mathcal{A}(w_n)\| = 0.$$

So, we have from Algorithm 1 that

$$\|z_{n+1} - w_n\| = \beta_n \|\mathcal{A}(z_n) - \mathcal{A}(w_n)\| \to 0, \quad n \to \infty.$$

Since $\{z_n\}$ is bounded, there exists a subsequence $\{z_{n_k}\} \subset \{z_n\}$ such that $z_{n_j} \rightharpoonup z \in \mathcal{H}, \ j \to \infty$. We show that $z \in \mathcal{S}$. By the definition of w_n, we have that $w_{n_j} = \Pi_C(\chi z_{n_j-1} + (1-\chi)z_{n_j} - \beta_{n_j}\mathcal{A}(z_{n_j}))$. By (1.2),

$$\langle \chi z_{n_j-1} + (1-\chi)z_{n_j} - w_{n_j} - \beta_{n_j}\mathcal{A}(z_{n_j}), y - w_{n_j}\rangle \leq 0, \ \forall\, y \in C,$$

and so

$$\frac{1}{\beta_{n_j}}\langle \chi z_{n_j-1} + (1-\chi)z_{n_j} - w_{n_j}, y - w_{n_j}\rangle \leq \langle \mathcal{A}(z_{n_j}), y - w_{n_j}\rangle, \ \forall\, y \in C.$$

Hence,

$$\frac{1}{\beta_{n_j}}\langle \chi z_{n_j-1} + (1-\chi)z_{n_j} - w_{n_j}, y - w_{n_j}\rangle + \langle \mathcal{A}(z_{n_j}), w_{n_j} - z_{n_j}\rangle \leq \langle \mathcal{A}(z_{n_j}), y - z_{n_j}\rangle \tag{3.18}$$

for all $y \in C$. Since $\{z_{n_j}\}$ is bounded, by the Lipschitz continuity of $\mathcal{A}$, we have that $\{\mathcal{A}(z_{n_j})\}$ is bounded. Moreover, $\lim_{j\to\infty} \|\chi z_{n_j-1} + (1-\chi)z_{n_j} - w_{n_j}\| = 0$ and the boundedness of $\{w_{n_j}\}$ imply that

$$\liminf_{k\to\infty}\langle \mathcal{A}(z_{n_j}), y - z_{n_j}\rangle \geq 0, \ \forall\, y \in C. \tag{3.19}$$

Consequently, the fact that $\lim_{i\to\infty} \|\mathcal{A}()w_{n_j}) - \mathcal{A}(z_{n_j})\| = 0$ and

$$\begin{aligned}\langle \mathcal{A}(w_{n_j}), y - w_{n_j}\rangle &= \langle \mathcal{A}(w_{n_j}) - \mathcal{A}(z_{n_j}), y - z_{n_j}\rangle + \langle \mathcal{A}(w_{n_j}), z_{n_j} - w_{n_j}\rangle \\ &\quad + \langle \mathcal{A}(z_{n_j}), y - z_{n_j}\rangle,\end{aligned} \tag{3.20}$$

yield

$$\liminf_{k\to\infty}\langle \mathcal{A}(w_{n_j}), y - w_{n_j}\rangle \geq 0, \quad \forall \quad y \in C.$$

Now, choose a sequence $\{\delta_k\}$ of positive numbers that is decreasing and $\delta_k \downarrow 0$. For each k, let N_k be the smallest positive integer such that

$$\langle \mathcal{A}(w_{n_r}), y - w_{n_r}\rangle + \delta_i \geq 0, \quad r \geq N_k. \tag{3.21}$$

Since $\{\delta_i\}$ is decreasing, we have $\{N_k\}$ is increasing. Furthermore, for each k, we can suppose that $Fw_{N_k} \neq 0$ (otherwise, w_{N_k} is a solution). Let $g_{N_k} = \frac{\mathcal{A}(w_{N_k})}{\|\mathcal{A}(w_{N_k})\|^2}$. We have $\langle Fw_{N_k}, g_{N_k}\rangle = 1$, for each k.

From (3.21), we have for each k that

$$\left\langle \mathcal{A}(w_{N_k}),\ y + \delta_k g_{N_k} - w_{N_k}\right\rangle \geq 0.$$

$\mathcal{A}$ being pseudo-monotone implies

$$\left\langle \mathcal{A}(y + \delta_k g_{N_k}),\ y + \delta_k g_{N_k} - w_{N_k}\right\rangle \geq 0.$$

Thus,

$$\left\langle \mathcal{A}(y),\ y - w_{N_k}\right\rangle \geq \left\langle \mathcal{A}(y) - \mathcal{A}(y + \delta_k g_{N_k}),\ y + \delta_k g_{N_k} - w_{N_k}\right\rangle - \delta_k\left\langle \mathcal{A}(y),\ g_{N_k}\right\rangle. \tag{3.22}$$

We now prove that $\lim_{k\to\infty} \delta_k g_{N_k} = 0$. Since $z_{n_j} \rightharpoonup z$ and $\lim_{k\to\infty} \|z_{n_j} - w_{n_j}\| = 0$, we have $w_{N_k} \rightharpoonup z$ as $k \to \infty$. Since $\{w_n\} \subset C$, we have $z \in C$. Since $\mathcal{A}$ satisfies Condition A, we have

$$0 < \|\mathcal{A}(z)\| \leq \liminf_{k\to\infty} \|\mathcal{A}(w_{n_j})\|.$$

Since $\{w_{N_k}\} \subset \{w_{n_j}\}$ and $\delta_k \to 0$ as $k \to \infty$, we obtain

$$0 \leq \limsup_{k\to\infty} \|\delta_k g_{N_k}\| = \limsup_{k\to\infty}\left(\frac{\delta_k}{\|\mathcal{A}(w_{n_j})\|}\right) \leq \frac{\limsup_{k\to\infty}\delta_k}{\liminf_{k\to\infty}\|\mathcal{A}(w_{n_j})\|} = 0,$$

and so $\lim_{k\to\infty} \delta_k g_{N_k} = 0$. Since $\mathcal{A}$ is Lipschitz continuous, $\{w_{N_k}\}$ and $\{g_{N_k}\}$ are bounded, and $\lim_{k\to\infty} \delta_k g_{N_k} = 0$, we obtain from (3.22) that

$$\liminf_{k\to\infty} \left\langle \mathcal{A}(y),\ y - w_{N_k}\right\rangle \geq 0.$$

Therefore, for all $y \in C$,

$$\langle \mathcal{A}(y),\, y - z \rangle = \lim_{k\to\infty} \langle \mathcal{A}(y),\, y - w_{N_k} \rangle = \liminf_{k\to\infty} \langle \mathcal{A}(x),\, y - w_{N_k} \rangle \geq 0.$$

We then obtain that $z \in \mathcal{S}$ by Lemma 2.2.

Now, define

$$b_n := \chi \|z_{n-1} - z_n\|^2 \to 0 \quad (n \to \infty),$$

and

$$c_n := 2\chi \langle z_{n-1} - z_n,\, z_n - x^* \rangle \to 0 \quad (n \to \infty),$$

since $\{z_n\}$ is bounded. Note that

$$\chi \|z_{n-1} - x^*\|^2 = \chi \|z_{n-1} - z_n\|^2 + 2\chi \langle z_{n-1} - z_n,\, z_n - x^* \rangle + \chi \|z_n - x^*\|^2,$$

and so

$$\begin{aligned} a_n &= \|z_n - x^*\|^2 + \chi \|z_{n-1} - x^*\|^2 \\ &= \|z_n - x^*\|^2 + \chi \|z_n - x^*\|^2 + \chi \|z_n - z_{n-1}\|^2 + 2\chi \langle z_{n-1} - z_n,\, z_n - x^* \rangle \\ &= (1+\chi)\|z_n - x^*\|^2 + \chi \|z_n - z_{n-1}\|^2 + 2\chi \langle z_{n-1} - z_n,\, z_n - x^* \rangle \\ &= (1+\chi)\|z_n - x^*\|^2 + b_n + c_n. \end{aligned}$$

Hence,

$$(1+\chi)\|z_n - x^*\|^2 = a_n - b_n - c_n. \tag{3.23}$$

Since $\lim_{n\to\infty} b_n = 0$, $\lim_{n\to\infty} c_n = 0$, and $\lim_{n\to\infty} a_n$ exists, we have that $\lim_{n\to\infty}(1+\chi)\|z_n - x^*\|^2$ exists. Now,

$$\lim_{n\to\infty} \|z_n - x^*\|^2 = \frac{1}{1+\chi} \lim_{n\to\infty} \left((1+\chi)\|z_n - x^*\|^2\right)$$

exists. We then obtain the weak convergence of $\{z_n\}$ by Lemma 2.1, and the weak convergence of $\{w_n\}$ follows immediately. □

Theorem 3.5. *Suppose that $\mathcal{A} : \mathcal{H} \to \mathcal{H}$ is ζ-strongly pseudo-monotone and L-Lipschitz continuous with constant $L > 0$. If $\beta_n = \beta \in \left(0, \frac{1}{\sqrt{2}L}\right)$, then the sequence $\{z_n\}$ converges at least linearly to the unique solution $x^* \in \mathcal{S}$.*

Proof. Since $x^* \in \mathcal{S}$, we have

$$\langle \mathcal{A}(x^*), w_n - x^* \rangle \geq 0.$$

Since $\mathcal{A}$ is ζ-strongly pseudo-monotone, it follows that

$$\langle \mathcal{A}(w_n), w_n - x^* \rangle \geq \zeta \|w_n - x^*\|^2. \tag{3.24}$$

Repeating the same line of reasoning from (3.3) to (3.15), we obtain

$$\begin{aligned} &\|z_{n+1} - x^*\|^2 + \chi \|z_n - x^*\|^2 \\ &\leq \|z_n - x^*\|^2 + \chi \|z_{n-1} - x^*\|^2 + \chi(2\chi - 1)\|z_n - z_{n-1}\|^2 \end{aligned}$$

$$-\left[\left(\frac{1}{2}-\beta^2L^2\right)\|w_n-z_n\|^2+2\zeta\beta\|w_n-x^*\|^2\right]. \tag{3.25}$$

Next, we estimate the terms involving w_n:

$$\|z_n-x^*\|^2=\|(z_n-w_n)+(w_n-x^*)\|^2\le 2\left(\|z_n-w_n\|^2+\|w_n-x^*\|^2\right).$$

Thus, we have the following inequality:

$$-\left(\|z_n-w_n\|^2+\|w_n-x^*\|^2\right)\le -\frac{1}{2}\|z_n-x^*\|^2.$$

Now, we estimate the remaining terms:

$$\begin{aligned}&\left[\left(\frac{1}{2}-\beta^2L^2\right)\|w_n-z_n\|^2+2\zeta\beta\|w_n-x^*\|^2\right]\\&\qquad\ge \min\left\{\frac{1}{2}-\beta^2L^2,2\zeta\beta\right\}\left(\|w_n-z_n\|^2+\|w_n-x^*\|^2\right).\end{aligned}$$

So, we obtain the following inequality:

$$\begin{aligned}&-\left[\left(\frac{1}{2}-\beta^2L^2\right)\|w_n-z_n\|^2+2\zeta\beta\|w_n-x^*\|^2\right]\\&\quad\le -\min\left\{\frac{1}{2}-\beta^2L^2,2\zeta\beta\right\}\left(\|w_n-z_n\|^2+\|w_n-x^*\|^2\right)\\&\quad\le -\frac{1}{2}\min\left\{\frac{1}{2}-\beta^2L^2,2\zeta\beta\right\}\|z_n-x^*\|^2.\end{aligned}$$

Plugging this into (3.25) gives:

$$\begin{aligned}\|z_{n+1}-x^*\|^2+\chi\|z_n-x^*\|^2 \quad\le\quad & \|z_n-x^*\|^2+\chi\|z_{n-1}-x^*\|^2\\&+\chi(2\chi-1)\|z_n-z_{n-1}\|^2\\&-\frac{1}{2}\min\left\{\frac{1}{2}-\beta^2L^2,2\zeta\beta\right\}\|z_n-x^*\|^2.\end{aligned}$$

Next, for any $r>0$, we obtain

$$\begin{aligned}\chi(2\chi-1)\|z_n-z_{n-1}\|^2 \quad&=\quad \chi(2\chi-1)\|z_n-x^*\|^2+\chi(2\chi-1)\|z_{n-1}-x^*\|^2\\&\qquad+2\chi(2\chi-1)\langle z_n-x^*,x^*-z_{n-1}\rangle\\&\le\quad \chi(2\chi-1)\|z_n-x^*\|^2+\chi(2\chi-1)\|z_{n-1}-x^*\|^2\\&\qquad-2\chi(2\chi-1)\|z_n-x^*\|\|x^*-z_{n-1}\|\\&\le\quad \chi(2\chi-1)\|z_n-x^*\|^2+\chi(2\chi-1)\|z_{n-1}-x^*\|^2\\&\qquad-r\chi(2\chi-1)\|z_n-x^*\|^2-\frac{1}{r}\chi(2\chi-1)\|z_{n-1}-x^*\|^2\\&=\quad \chi(2\chi-1)(1-r)\|z_n-x^*\|^2\end{aligned}$$

$$+\chi(2\chi-1)\left(1-\frac{1}{r}\right)\|z_{n-1}-x^*\|^2.$$

Thus, we have the following inequality:

$$\begin{aligned}&\|z_{n+1}-x^*\|^2+\chi\|z_n-x^*\|^2\\ \leq\ &\left(1+\chi(2\chi-1)(1-r)-\frac{1}{2}\min\left\{\frac{1}{2}-\beta^2L^2,2\zeta\beta\right\}\right)\|z_n-x^*\|^2\\ &+\chi\left(1+(2\chi-1)\left(1-\frac{1}{r}\right)\right)\|z_{n-1}-x^*\|^2.\end{aligned}$$

Note that for $r\in\left(1,1-\frac{c}{2\chi(2\chi-1)}\right)$, where $c:=\frac{1}{2}\min\left\{\frac{1}{2}-\beta^2L^2,2\zeta\beta\right\}$, we have

$$\tilde{c}:=\max\left\{1+(2\chi-1)\left(1-\frac{1}{r}\right),1+\chi(2\chi-1)(1-r)-c\right\}\in(0,1).$$

Thus, we obtain the following inequality:

$$\|z_{n+1}-x^*\|^2+\chi\|z_n-x^*\|^2\leq\tilde{c}\left(\|z_n-x^*\|^2+\chi\|z_{n-1}-x^*\|^2\right),$$

which inductively implies that

$$\|z_{n+1}-x^*\|^2+\chi\|z_n-x^*\|^2\leq\tilde{c}^n\left(\|z_1-x^*\|^2+\chi\|z_0-x^*\|^2\right).$$

Therefore, the sequence $\{z_n\}$ converges (at least) linearly to x^*. □

Having proved the convergence properties of the algorithm, the next section illustrates its practical behavior on a blood supply chain network.

4. The setting of blood supply chain network

Following the network architecture introduced in [69], we present in Figure 1 a schematic illustration of the blood supply chain and introduce the associated mathematical formulation. This class of network equilibrium models for blood logistics has been extensively investigated; see [56, 59, 69] and related works for comprehensive discussions.

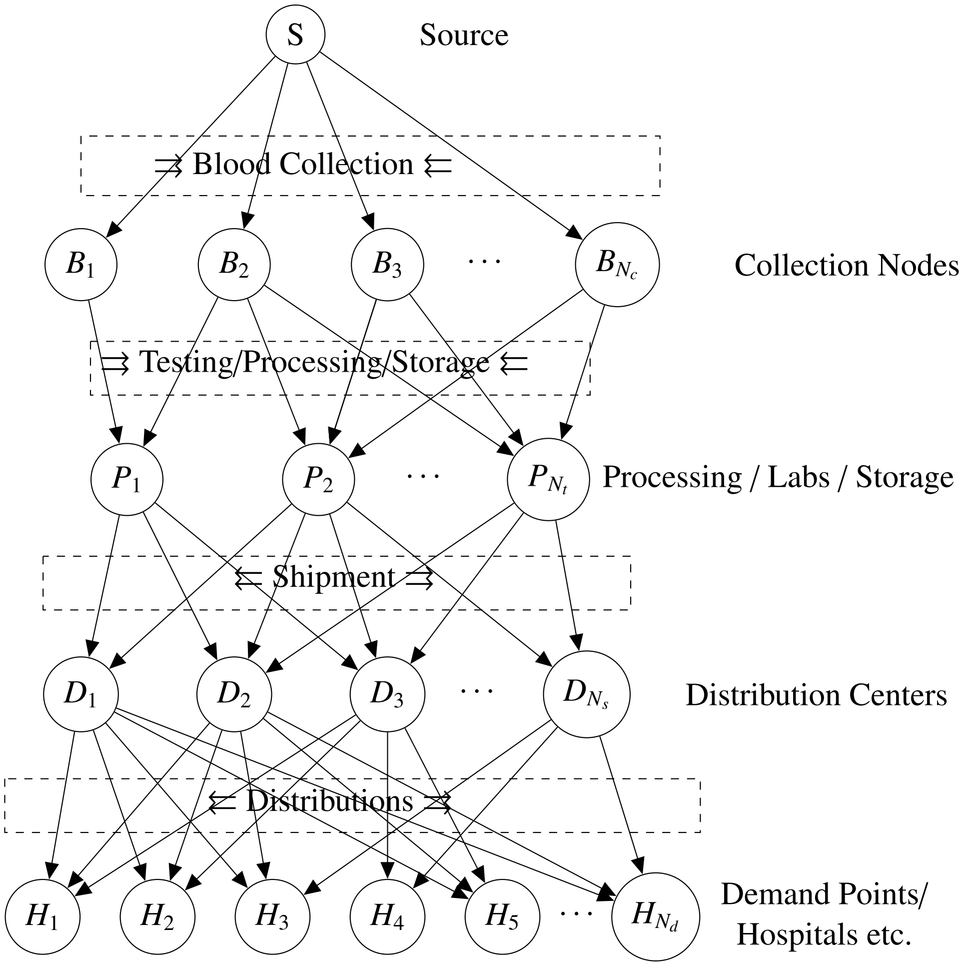

Figure 1. Blood supply network topology [69].

The scenario considered, shown in Figure 1, is a multi-echelon blood supply chain comprising of four tiers: Collection centers (blood drives), processing and testing facilities, distribution centers, and hospitals (demand points). Blood products are perishable and subject to losses at each stage. The decision maker must determine the optimal flow of blood from collection to hospitals to minimize total cost, including operational, disposal, and shortage costs, while respecting capacity constraints and uncertain demand. This problem is formulated as a variational inequality.

The network in Figure 1 represents the movement of blood products from collection facilities to processing units, then to distribution centers, and finally to hospitals. Let N_{cf}, N_{pu}, N_{sd}, and N_{dl} denote the numbers of collection, processing, distribution, and demand nodes, respectively. The set of admissible routes is $\{\rho_\ell : \ell \in \mathcal{R}\}$, where $\mathcal{R}$ indexes all routes, and x_ℓ denotes the flow assigned to route ρ_ℓ.

We define the feasible paths by $\mathcal{P} = \{p_k : k \in \mathcal{K}\}$, where each path p_k corresponds to a directed chain from a collection node to a hospital. The decision variable y_k represents the initial flow injected into path p_k. The objective is to determine an optimal feasible vector $\mathbf{y}^* = (y_k^*, k \in \mathcal{K})$ that balances cost, risk, and demand satisfaction.

Blood handling at each stage may result in unavoidable losses due to testing, processing, or expiration. To model this effect, each route ρ_ℓ is assigned a retention coefficient $\theta_\ell \in (0, 1]$, assumed to be independent of the flow magnitude. Consequently, an inflow x_ℓ yields an effective output of $\theta_\ell x_\ell$, while the discarded quantity is $(1-\theta_\ell)x_\ell$.

Let $\alpha_\ell(x_\ell)$ and $\beta_\ell(x_\ell)$ denote the unit operational and disposal costs on route ρ_ℓ, respectively. The corresponding total is computed by

$$\widetilde{\alpha}_\ell(x_\ell) = x_\ell \alpha_\ell(x_\ell), \qquad \widetilde{\beta}_\ell(x_\ell) = x_\ell \beta_\ell(x_\ell).$$

Aggregating these costs across the network yields the total operational-disposal cost function

$$\Psi_1(\mathbf{x}) := \sum_{\ell \in \mathcal{R}} x_\ell\big(\alpha_\ell(x_\ell) + \beta_\ell(x_\ell)\big), \quad \mathbf{x} = (x_\ell, \ell \in \mathcal{R}).$$

For each feasible path p_k, the cumulative survival factor is defined as

$$\omega_k = \prod_{\ell:\rho_\ell \in p_k} \theta_\ell.$$

Thus, an initial flow y_k generates a delivered quantity $\omega_k y_k$. The total supply delivered to demand node H_m is therefore

$$q_m = \sum_{k:p_k \in \mathcal{P}_m} \omega_k y_k,$$

where $\mathcal{P}_m$ denotes the set of paths terminating at H_m. The realized demand at H_m is uncertain and modeled as a random variable ξ_m with probability density function g_m. Its cumulative distribution function is

$$\mathbb{P}_m(z) = \mathrm{Prob}(\xi_m < z) = \int_0^z g_m(s)\, ds.$$

At each demand node, shortages and surpluses are quantified by

$$S_m = \max\{0, \xi_m - q_m\}, \qquad E_m = \max\{0, q_m - \xi_m\}, \quad m \in \mathcal{D},$$

where $\mathcal{D}$ is the index set of demand nodes. Their expected values are

$$\mathbb{E}(S_m) = \int_{q_m}^{\infty} (s - q_m) g_m(s)\, ds, \qquad \mathbb{E}(E_m) = \int_0^{q_m} (q_m - s) g_m(s)\, ds.$$

Given the societal importance of timely blood availability, shortages incur a severe penalty $\pi_m^{(1)}$, reflecting health and social consequences. Conversely, excess supply results in wastage penalties $\pi_m^{(2)}$ due to perishability and disposal costs; see [56, 75]. The expected penalty at node H_m is thus

$$\mathbb{E}(\pi_m^{(1)} S_m + \pi_m^{(2)} E_m) = \pi_m^{(1)}\mathbb{E}(S_m) + \pi_m^{(2)}\mathbb{E}(E_m),$$

and the aggregate penalty across all demand nodes is

$$\Psi_2(\mathbf{x}) := \sum_{m \in \mathcal{D}} \left(\pi_m^{(1)}\mathbb{E}(S_m) + \pi_m^{(2)}\mathbb{E}(E_m)\right).$$

Due to the sequential organization of the network, routes can be indexed so that downstream routes always have larger indices than upstream ones. Under this convention, the flow on route ρ_ℓ can be expressed in terms of path flows as

$$x_\ell = \sum_{k:\rho_\ell \in p_k} \kappa_{\ell k} y_k,$$

where

$$\kappa_{\ell k} = \begin{cases} \delta_{\ell k} \prod\limits_{r \in \mathcal{S}_{\ell k}} \theta_r, & \mathcal{S}_{\ell k} \neq \emptyset, \\ \delta_{\ell k}, & \mathcal{S}_{\ell k} = \emptyset, \end{cases}$$

$\mathcal{S}_{\ell k}$ denotes the set of routes preceding ρ_ℓ along p_k, and $\delta_{\ell k} = 1$ if $\rho_\ell \in p_k$ and 0 otherwise.

In addition to cost considerations, supply uncertainty, particularly at collection facilities, introduces significant operational risk. Following [56,76], we associate a unit risk function r_h with each collection route and define the total risk contribution accordingly. A risk sensitivity parameter $\gamma > 0$ is introduced to reflect the decision-maker's attitude toward uncertainty.

The overall objective function can thus be written as

$$\Phi(\mathbf{y}) = \sum_{k \in \mathcal{K}} (A_k(\mathbf{y}) + B_k(\mathbf{y}) + \gamma R_k(\mathbf{y})) + \sum_{m \in \mathcal{D}} \left(\pi_m^{(1)} \mathbb{E}(S_m) + \pi_m^{(2)} \mathbb{E}(E_m) \right),$$

where

$$A_k(\mathbf{y}) = y_k \sum_{\ell \in \mathcal{R}} \kappa_{\ell k} \alpha_\ell(x_\ell), \quad B_k(\mathbf{y}) = y_k \sum_{\ell \in \mathcal{R}} \kappa_{\ell k} \beta_\ell(x_\ell), \quad R_k(\mathbf{y}) = y_k \sum_{\ell \in C} \kappa_{\ell k} r_\ell(x_\ell),$$

and C denotes the index set of collection routes. The feasibility condition requires

$$y_k \geq 0, \qquad k \in \mathcal{K}.$$

Assuming that A_k, B_k, and R_k are convex and continuously differentiable, minimizing Φ is equivalent to the following variational inequality: Find $\mathbf{y}^* \in \mathbb{R}_+^{|\mathcal{K}|}$ such that

$$\sum_{k \in \mathcal{K}} (y_k - y_k^*) \mathcal{A}_k(\mathbf{y}^*) \geq 0, \qquad \forall\, \mathbf{y} \in \mathbb{R}_+^{|\mathcal{K}|},$$

where $\mathcal{A}_k(\mathbf{y}) = \frac{\partial \Phi(\mathbf{y})}{\partial y_k}$. The explicit form of $\mathcal{A}_k$ follows directly from the chain rule and the representation of x_ℓ in terms of path flows; see [56] for further details.

The cost functions $\alpha_\ell(x_\ell)$ and $\beta_\ell(x_\ell)$ represent, respectively, the unit operational and disposal costs along route ℓ. The retention coefficient θ_ℓ models the fraction of blood that survives testing and handling. The expected shortage and surplus penalties, $\pi_m^{(1)} \mathbb{E}(S_m) + \pi_m^{(2)} \mathbb{E}(E_m)$, capture the societal cost of blood unavailability and the wastage cost of excess supply. By imposing suitable conditions on A_k, B_k, or R_k, the resulting operator $\mathcal{A}$ can be pseudo-monotone, reflecting the fact that the overall cost function is generally not convex due to asymmetric congestion effects and interactions among echelons.

For the purpose of numerical illustration, primarily to showcase the performance of the proposed algorithm relative to benchmark methods, we consider settings in which the objective functions are convex, ensuring that the mapping is pseudo-monotone and, in fact, monotone. Cases involving non-monotone pseudo-monotone operators are instead addressed in Example 5.1.

4.1. Numerical illustrations

Consider the blood supply network depicted in Figure 2, consisting of two collection points (B_1, B_2), two processing and storage facilities (P_1, P_2), two distribution nodes (D_1, D_2), and three demand points (H_1, H_2, H_3). The four layers correspond directly to the echelons described in the model: Collection nodes (Layer 1) represent the sources of blood; processing nodes (Layer 2) perform testing and conversion; distribution nodes (Layer 3) act as intermediate warehouses; and demand nodes (Layer 4) are hospitals with stochastic demand.

The network topology generates a total of 24 feasible paths, categorized according to the demand nodes as follows:

$$\begin{aligned}
\mathcal{P}_1 = \Big\{&[1,3,7,11],[1,3,8,14],[1,4,9,11],[1,4,10,14],\\
&[2,5,7,11],[2,5,8,14],[2,6,9,11],[2,6,10,14]\Big\},\\
\mathcal{P}_2 = \Big\{&[1,3,7,12],[1,3,8,15],[1,4,9,12],[1,4,10,15],\\
&[2,5,7,12],[2,5,8,15],[2,6,9,12],[2,6,10,15]\Big\},\\
\mathcal{P}_3 = \Big\{&[1,3,7,13],[1,3,8,16],[1,4,9,13],[1,4,10,16],\\
&[2,5,7,13],[2,5,8,16],[2,6,9,13],[2,6,10,16]\Big\}.
\end{aligned}$$

Here, $\mathcal{P}_k$ denotes the set of paths terminating at demand node H_k, for $k = 1, 2, 3$.

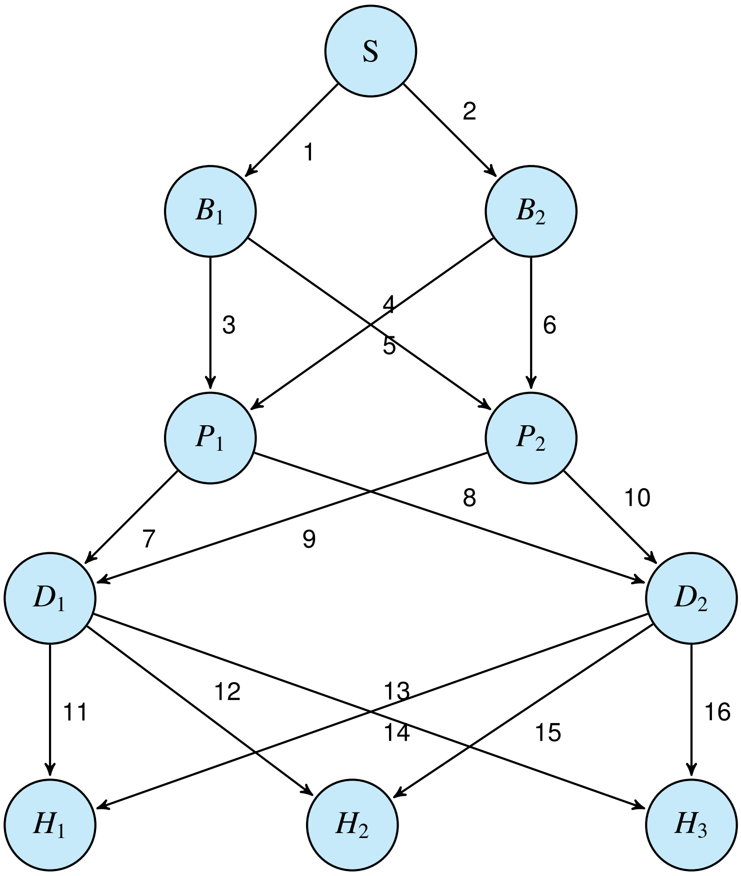

Figure 2. Blood supply network topology. Layer 1: two collection centers B_1, B_2; Layer 2: two processing/storage facilities P_1, P_2; Layer 3: two distribution nodes D_1, D_2; Layer 4: three demand points (hospitals) H_1, H_2, H_3. Each directed path from a source to a demand node represents a feasible route for blood flow [69].

For the demand profile, we assume that H_2 corresponds to a major surgical center with the highest blood requirements, followed by H_3, and finally H_1 with comparatively lower demand. The demands at each node are modeled using uniform distributions over $[5,20]$, $[55,80]$, and $[35,65]$ for H_1, H_2, and H_3, respectively. Formally, the probability distribution for the demand ξ_k at node H_k is given by

$$\mathbb{P}_{m_k}\left(\sum_{i:\bar{I}_i\in\mathcal{L}_k}\xi_i f_i\right)=\frac{1}{b_k}\left(\sum_{i:\bar{I}_i\in\mathcal{L}_k}\xi_i f_i-a_k\right),\quad k=1,2,3,$$

with $a_1=5, b_1=15$, $a_2=55, b_2=25$, and $a_3=35, b_3=30$.

Operational risk associated with collection routes is included in all experiments as

$$\check{r}_1(x_1)=2x_1^2,\qquad \check{r}_2(x_2)=\frac{3}{2}x_2^2.$$

We also introduce the following residual metric to monitor convergence:

$$\mathrm{Res}_n^{(2)}=\left\|w_{n+1}-\Pi_C\big(w_{n+1}-\beta^*\mathcal{A}(w_{n+1})\big)\right\|.$$

To evaluate the numerical performance of Algorithm 1 in a supply chain network, as depicted in Figure 2, we adopt the settings described and compare them with related schemes known for such optimization tasks. The proposed algorithm, denoted by `PrpALg`, is evaluated alongside two other schemes: `SpkALg` (as presented in (1.6)) and a variant of [19], denoted `PpvALg`, which operates with the following initial conditions: $z_0, w_0\in C$, $\sigma\in(0,1/3)$, and $\beta_0>0$. The iterative scheme for `PpvALg` is given by:

$$z_{n+1}=\Pi_C\left(z_n-\beta_n\mathcal{G}(w_n)\right),\quad w_{n+1}=\Pi_C\left(z_{n+1}-\beta_n\mathcal{G}(w_n)\right).$$

We also include the adaptive scheme from [24], denoted `MalALg`, which uses initial values $w_0, w_1\in C$, $\sigma\in(0,1/2)$, and $\beta_0,\beta_1>0$, iterating according to:

$$w_{n+1}=\Pi_C\left(w_n-\beta_n\mathcal{G}(w_n)-\beta_{n-1}\left(\mathcal{G}(w_n)-\mathcal{G}(w_{n-1})\right)\right).$$

The stepsize for both algorithms is updated using the adaptive rule:

$$\beta_{n+1}=\min\left\{\beta_n,\sigma\frac{\|w_{n+1}-w_n\|}{\|\mathcal{G}(w_{n+1})-\mathcal{G}(w_n)\|}\right\}.$$

In the MATLAB implementation, `PrpALg` is set with parameters $\chi=0.0001$ and $\sigma=0.707$, and the residual error criterion $\mathrm{Res}_n^{(1)}=\|w_{n+1}-z_{n+1}\|^2+\|z_{n+1}-w_n\|^2$. For `SpkALg`, we use $\xi_n=\frac{1}{(1+n)^{1.00001}\|d_n\|}$, with $\sigma=0.9$, and the residual error $\mathrm{Res}_n^{(1)}=\|w_{n+1}-z_n\|^2+\|z_n-w_n\|^2$. For `PpvALg`, the parameters are $\sigma=0.25$, and the residual error $\mathrm{Res}_n^{(1)}=\|w_{n+1}-z_{n+1}\|^2+\|z_{n+1}-z_n\|^2$. For `MalALg`, the parameters are $\sigma=0.45$, and the error criterion $\mathrm{Res}_n^{(1)}=\|w_{n+1}-w_n\|^2+\|w_n-w_{n-1}\|^2$. The initial iterate w_0 is randomly generated from a uniform distribution on the interval $[0,1]$, and the initial step sizes are set as $\beta_0=\beta_1=1$.

For each method, the optimal flows, total cost, and waste are recorded once 500 iterations have been completed. The experiment is conducted across three distinct cases, each with different sets of flow and waste costs, as well as varying route multipliers:

- **Case 1:** The risk-aversion coefficient is set to $\gamma = 0.7$, with shortages and surpluses for the three demand nodes specified as:

$$S_m^{(1)} = 2800,\ \ S_m^{(2)} = 2000,\ \ S_m^{(3)} = 2500, \quad E_m^{(1)} = 80,\ \ E_m^{(2)} = 60,\ \ E_m^{(3)} = 100.$$

The results of this experiment are presented in Figure 3, which shows the residual decays, and in Table 2, which displays the distinct values of the flow and waste cost functions along with the corresponding route multipliers. The table also presents the obtained expected demand values and the optimal flow for each route.

- **Case 2:** The risk-aversion coefficient is set to $\gamma = 0.8$, with shortages and surpluses for the three demand nodes specified as

$$S_m^{(1)} = 2800,\ \ S_m^{(2)} = 2000,\ \ S_m^{(3)} = 2500, \quad E_m^{(1)} = 50,\ \ E_m^{(2)} = 60,\ \ E_m^{(3)} = 50.$$

The results of this experiment are presented in Figure 4, which shows the residual decays, and in Table 3 which presents similar terms to those in Table 2 but with distinct values.

- **Case 3:** The risk-aversion coefficient is set to $\gamma = 0.5$, with shortages and surpluses for the three demand nodes specified as

$$S_m^{(1)} = 2900,\ \ S_m^{(2)} = 3000,\ \ S_m^{(3)} = 300, \quad E_m^{(1)} = 60,\ \ E_m^{(2)} = 70,\ \ E_m^{(3)} = 50.$$

The results of this experiment are presented in Figure 5, which shows the residual decays, and in Table 4, which presents similar terms to those in Table 2 but with distinct values.

Remark 4.1. The step-size parameter σ is chosen individually for each algorithm within its admissible convergence range. Since different algorithms have distinct parameter constraints and sensitivities, selecting a common fixed value of σ may lead to suboptimal or even invalid performance for some methods. Therefore, σ is tuned separately to ensure a fair and meaningful comparison. Numerical experiments indicate that the relative performance of the algorithms remains consistent under moderate variations of higher values of σ within the feasible range.

Following the results obtained in Figures 3–5 and Tables 2–4, it is evident that Algorithm 1 performs reasonably and comparatively well, demonstrating promise in the context of blood supply chain networks among other problems. Notably, the compared algorithms are recognized as the best performers in this type of supply chain network, as recorded in [59, 69]. Furthermore, the results clearly show that the expected demand values remained within the acceptable uniform ranges, even before 500 iterations. Therefore, the proposed algorithm not only works effectively for cases involving pseudo-monotone operators that are not necessarily monotone, but it also appears to be competitive and promising, even among algorithms for the monotone class of operators.

The encouraging results on the supply chain application motivate further testing on standard benchmark problems, which we present next.

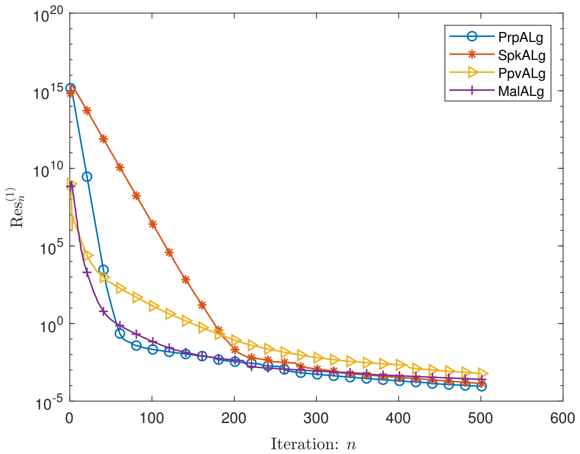

(a) $\mathrm{Res}_n^{(1)}$ vs. Iteration

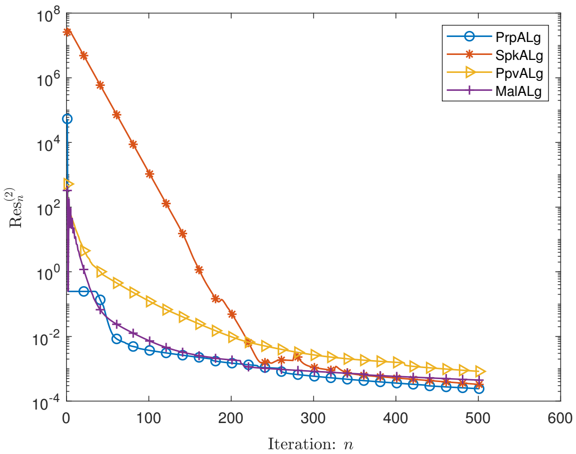

(b) $\mathrm{Res}_n^{(2)}$ vs. Iteration

Figure 3. Residual decay of the four algorithms for convergence in Case 1.

Table 2. Total supply cost $\widetilde{\alpha}_\ell(u_\ell) = a_\ell u_\ell^2 + b_\ell u_\ell$, waste cost $\widetilde{\beta}_\ell(u_\ell) = c_\ell u_\ell^2$, route multipliers θ_ℓ, and optimal route values (i.e., the equilibrium flows x_ℓ obtained as the solution of the variational inequality) for each algorithm based on Case 1.

ρ_ℓ	θ_ℓ	a_ℓ	b_ℓ	c_ℓ	PrpALg	SpkALg	PpvALg	MalALg
1	1	13	13	0.8	35.9489	35.90412	35.24464	35.58818
2	0.79	2.9	8	0.7	67.47724	67.52288	66.73232	67.82186
3	1	5.3	9	0.6	0	-0.00037	0	0
4	0.99	1.2	12	0.8	35.9489	3.59E+01	35.24464	35.58818
5	1	1	3	0.6	50.41729	5.04E+01	50.95778	50.72208
6	0.67	8.6	2	0.8	2.889733	2.963634	1.760759	2.857194
7	0.62	4	8	0.3	7.985935	7.82899	5.306275	8.513018
8	0.96	5	2	0.4	42.43135	42.55008	45.6515	42.20906
9	0.8	0.4	7	0.3	19.82526	19.93707	17.50856	18.19853
10	1	6	1	0.4	17.70027	1.76E+01	18.56334	18.94809
11	0.24	7.3	6	0.7	0	-5.53E-05	0	0
12	1	3	2	0.4	20.81149	20.8037	17.29674	19.83689
13	0.28	5.5	5	0.5	0	-1.75E-05	0	0
14	1	8.7	2	0.7	7.04358	7.030722	7.04847	7.023714
15	0.91	2.6	8	0.4	22.16801	2.22E+01	26.10893	23.24049
16	1	4.1	2	0.5	29.22279	2.92E+01	29.23139	29.20458
Expected demands				q_1^*	7.04358	7.030708374	7.04847	7.023714
				q_2^*	40.98438	40.98925242	41.05586	40.98574
				q_3^*	29.22279	29.22943791	29.23139	29.20458

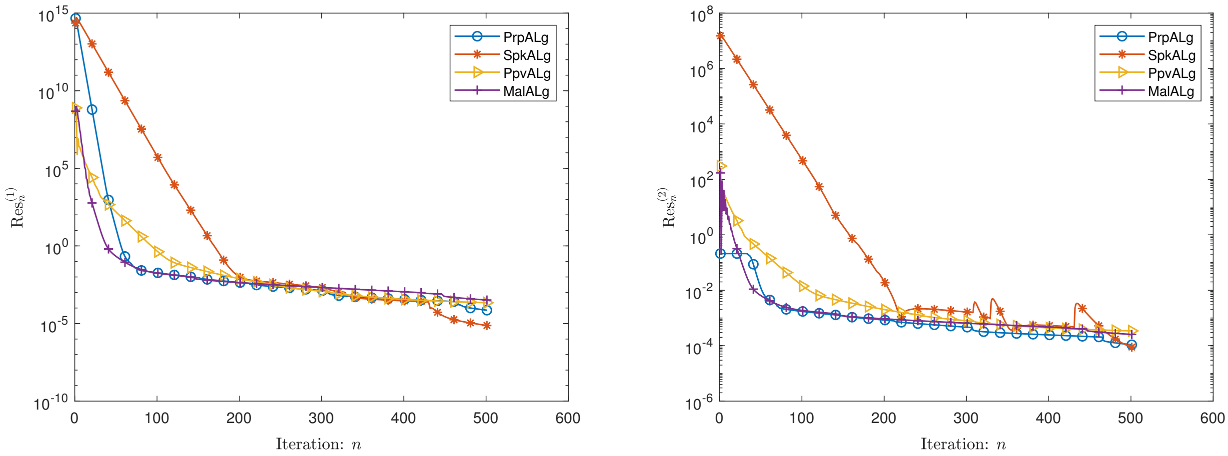

(a) $\mathrm{Res}_n^{(1)}$ vs. Iteration **(b)** $\mathrm{Res}_n^{(2)}$ vs. Iteration

Figure 4. Residual decay of the four algorithms for convergence in Case 2.

Table 3. Total supply cost $\widetilde{\alpha}_\ell(u_\ell) = a_\ell u_\ell^2 + b_\ell u_\ell$, waste cost $\widetilde{\beta}_\ell(u_\ell) = c_\ell u_\ell^2$, route multipliers θ_ℓ, and optimal route values for each algorithm based on Case 2.

ρ_ℓ	θ_ℓ	a_ℓ	b_ℓ	c_ℓ	PrpALg	SpkALg	PpvALg	MalALg
1	0.77	7	15	0.8	32.81036	32.52095	32.0772	32.74174
2	0.99	2	11	0.7	69.3699	69.36818	69.76203	69.40171
3	1	3.7	1	0.6	0	-0.00012	0	0
4	0.99	1.2	1	0.8	25.26398	2.50E+01	24.69944	25.21114
5	1	1	3	0.6	64.93755	6.52E+01	65.97183	64.83477
6	0.67	8	2	0.7	3.738652	3.438511	3.092579	3.872927
7	0.92	4	1	0.3	35.86728	3.67E+01	39.38681	36.45648
8	0.96	5	2	0.5	29.07027	28.49907	26.58502	28.37828
9	0.8	0.4	2	0.3	11.96486	10.96503	10.76215	11.76502
10	1	6	1	0.4	15.55137	1.61E+01	15.76232	15.78887
11	0.24	1.3	3	0.3	0	-1.68E-05	0	0
12	1	3	2	0.4	42.56979	42.56993	42.51272	42.55298
13	0.98	0.5	3	0.2	0	-4.37E-05	2.332871	0.399
14	0.7	0.7	2	0.6	10.00042	10.01207	10.07456	10.01594
15	0.11	0.6	4	0.4	0	-3.71E-05	0	0
16	0.98	0.1	5	0.1	33.45841	3.35E+01	31.20938	33.01609
Expected demands				q_1^*	7.000295	7.008442	7.052194	7.011155
				q_2^*	42.56979	42.56993	42.51272	42.55298
				q_3^*	32.78924	32.80712	32.8714	32.74678

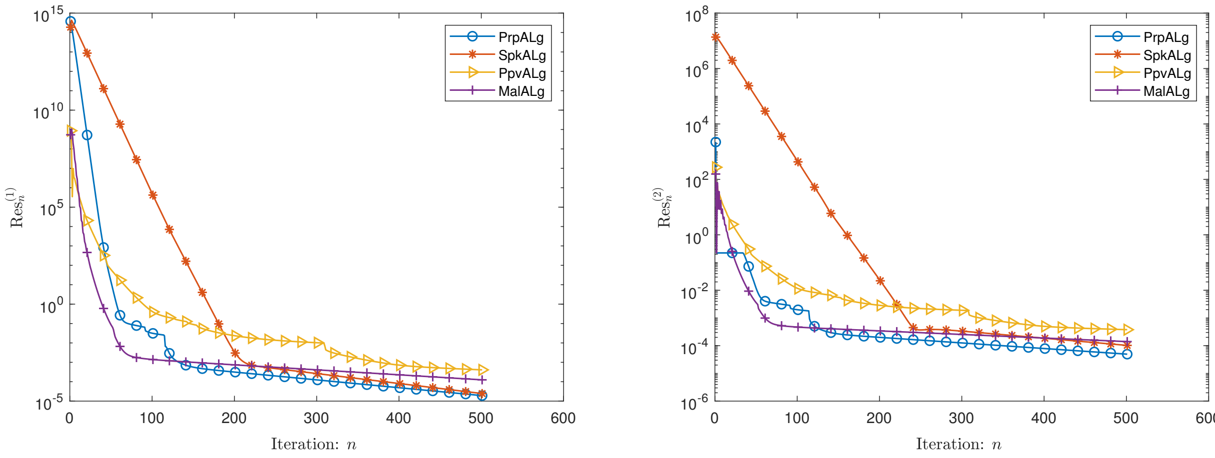

(a) $\mathrm{Res}_n^{(1)}$ vs. Iteration **(b)** $\mathrm{Res}_n^{(2)}$ vs. Iteration

Figure 5. Residual decay of the four algorithms for convergence in Case 3.

Table 4. Total supply cost $\widetilde{\alpha}_\ell(u_\ell) = a_\ell u_\ell^2 + b_\ell u_\ell$, waste cost $\widetilde{\beta}_\ell(u_\ell) = c_\ell u_\ell^2$, route multipliers θ_ℓ, and optimal route values for each algorithm based on Case 3.

ρ_ℓ	θ_ℓ	a_ℓ	b_ℓ	c_ℓ	PrpALg	SpkALg	PpvALg	MalALg
1	0.97	6	12	0.7	60.24931	60.23908	60.89652	60.41836
2	0.99	9	13	0.6	48.17792	48.1808	47.97685	48.13273
3	1	1.7	3	0.8	26.38897	26.32711	30.02493	27.39191
4	0.99	3.2	4	0.5	32.05286	3.21E+01	29.0447	31.2139
5	1	1	3	0.2	30.97609	3.10E+01	27.29733	29.9611
6	0.87	0.7	2	0.6	16.72004	16.66009	20.19975	17.6903
7	0.72	3	5	0.4	57.36506	5.74E+01	57.32226	57.35301
8	0.36	6	2	0.7	0	9.53E-05	0	0
9	0.48	0.4	4	0.5	0	2.33E-05	0	0
10	1	4	3	0.4	46.27877	4.63E+01	46.32803	46.29232
11	0.54	1.3	2	0.1	0	5.64E-05	0	0
12	1	6	2	0.3	41.30284	41.30339	41.27203	41.29417
13	0.48	0.3	1	0.3	0	2.25E-05	0	0
14	0.6	0.6	2	0.5	8.731806	8.731576	8.749704	8.736732
15	0.31	0.8	4	0.7	0	6.32E-06	0	0
16	0.78	0.11	3	0.2	37.54696	3.75E+01	37.57833	37.55559
Expected demands				q_1^*	5.239084	5.238976	5.249822	5.242039
				q_2^*	41.30284	41.30339	41.27203	41.29417
				q_3^*	29.28663	29.28625	29.3111	29.29336

5. Additional numerical results

In this section, we present the implementation and numerical performance of Algorithm 1 applied to certain test function. Its performance is then compared with several well-established methods from the same class in order to assess the effectiveness, computational efficiency, and accuracy of the algorithm.

Example 5.1. *Consider the operator $\mathcal{A} : \mathbb{R}^m \to \mathbb{R}^m$ defined by*

$$\mathcal{A}(w) := (e^{-w^\top M w} + \xi)\,(Hw + p),$$

where $M \in \mathbb{R}^{m\times m}$ is a symmetric positive definite matrix, $H \in \mathbb{R}^{m\times m}$ is symmetric and positive semi-definite, $p \in \mathbb{R}^m$ is a given vector, and $\xi > 0$ is a positive real number. As shown in [42, Example 2.1], the operator $\mathcal{A}$ is pseudo-monotone and satisfies a Lipschitz-type continuity condition.

For the numerical implementation, the problem dimension is fixed at $m = 40$. The initial iterates $z_0 = z_1 \in \mathbb{R}^m$ are generated randomly, with each component uniformly distributed over the interval $[-1, 1]$. The initial step size is set to $\beta_1 = 0.001$. The matrix M is chosen as

$$M = Q^\top Q + 2I_m,$$

where $Q \in \mathbb{R}^{m\times m}$ is a randomly generated matrix, ensuring that M is positive definite. Similarly, the matrix H is defined by

$$H = B^\top B,$$

with $B \in \mathbb{R}^{m\times m}$ chosen at random, which guarantees that H is positive semi-definite. The vector p is generated randomly in $[0, 1]$, and the parameter ξ is selected uniformly from the interval $[5, 6]$.

The feasible set is taken to be a polyhedral subset of $\mathbb{R}^m$ defined by

$$C := \{x \in \mathbb{R}^m \,\big|\, B_{\text{proj}} x \le b_{\text{proj}}\},$$

where $B_{\text{proj}} \in \mathbb{R}^{l\times m}$ is a randomly generated matrix with entries uniformly distributed in $[-1, 1]$ and $b_{\text{proj}} = (10, 10, \ldots, 10)^\top \in \mathbb{R}^l$ is a constant vector.

Numerical results are reported for up to 300 iterations in order to examine the influence of the parameters χ and σ. The projection onto the feasible set C is implemented to enforce the linear inequality constraints $B_{\text{proj}} x \le b_{\text{proj}}$. Convergence behavior is assessed using the residual measure

$$\text{Res}(w) := \left\| w - \Pi_C(w - \varepsilon\mathcal{A}(w)) \right\|^2, \quad \varepsilon = 10^{-4},$$

which serves as the primary indicator of the algorithm's performance.

Based on Example 5.1, Figure 6 indicates that smaller values of χ lead to faster convergence, as evidenced by a more rapid decay of the residual Res. In addition, larger values of σ appear to further enhance the convergence behavior. These observations naturally raise the following question: Is it possible to allow σ to be greater than or equal to $1/\sqrt{2}$, and if so, would such a choice result in additional acceleration of the algorithm? Furthermore, it is of interest to investigate whether the observed performance pattern persists for problems other than the test case in Example 5.1. A related and important question is whether the influence of these parameters can be theoretically justified, rather than being supported solely by empirical evidence.

To assess the effectiveness of the proposed approach applied to Example 5.1, we analyze it against five recently developed methods that have demonstrated strong empirical performance, including schemes incorporating inertial or extrapolation techniques. For each competing method, the algorithmic parameters are chosen in accordance with the convergence requirements specified in the respective original studies.

The proposed method, denoted by `PrpALg`, corresponds to Algorithm 1, with parameters selected as $\chi = 0.0001$ and $\sigma = 0.707$. It is compared with the golden ratio algorithm of Malitsky, referred to as `MlkALg`, which employs the golden ratio constant $\phi = (1 + \sqrt{5})/2$ and an upper step-size bound $\bar{\lambda} = 10^5$. Then, the forward–backward–forward scheme with relaxation, labeled `BotAlg` corresonding to Algorithm 3.1 in [42], is implemented with the fixed parameter $\rho_n = 10^{-5}$. We also include a modified Tseng-type method with extrapolation from previous iterates, denoted `TngAlg`, based on Algorithm (3.1) in [77] and using the adaptive strategy described therein with $\mu = 0.49$.

In addition, the single-projection method with double inertial extrapolation proposed in [54], referred to as `ThnAlg`, is tested using the parameter choices $\alpha = 0.45, \beta = 0.93, \theta = 0.35, \mu = 0.9$, and $\alpha_n = 1/n^2$. Finally, Tseng's splitting algorithm with two inertial terms from [50], labeled `WngAlg`, is implemented with parameters $\alpha_n = 1 - 10^{-n}$, $\beta_n = 0.1 - (1000 + n)^{-1}$, $\mu_n = 0$, $\mu = 0.9$, $p_n = 1/n^2$, and $\theta_n = 0.45 - (1000 + n)^{-1}$. All algorithms are initialized with the same starting points $z_0 = z_1 \in \mathbb{R}^m$, which are generated randomly in the same manner as in Figure 6, with each component drawn from the interval $[-1, 1]$. Moreover, all step sizes are initialized uniformly with the common value $\beta_1 = 0.001$. Nevertheless, the reported figures correspond to problems of varying dimensions and constraint structures, which are deliberately chosen to demonstrate that the effectiveness of the proposed algorithm is essentially independent of the dimensionality of the underlying problem.

It is evident from the numerical results obtained across four different problem dimensions (Figures 7–10) that the residual decay produced by Algorithm 1 is highly competitive when compared with that of the other five algorithms. In addition, the proposed Algorithm 1 consistently achieves the lowest execution time among all the methods considered while remaining closely comparable to Tseng's splitting algorithm with double inertial terms reported in [50]. Overall, these observations indicate that the proposed algorithm demonstrates strong efficiency and reliable performance for implementation and adaptability.

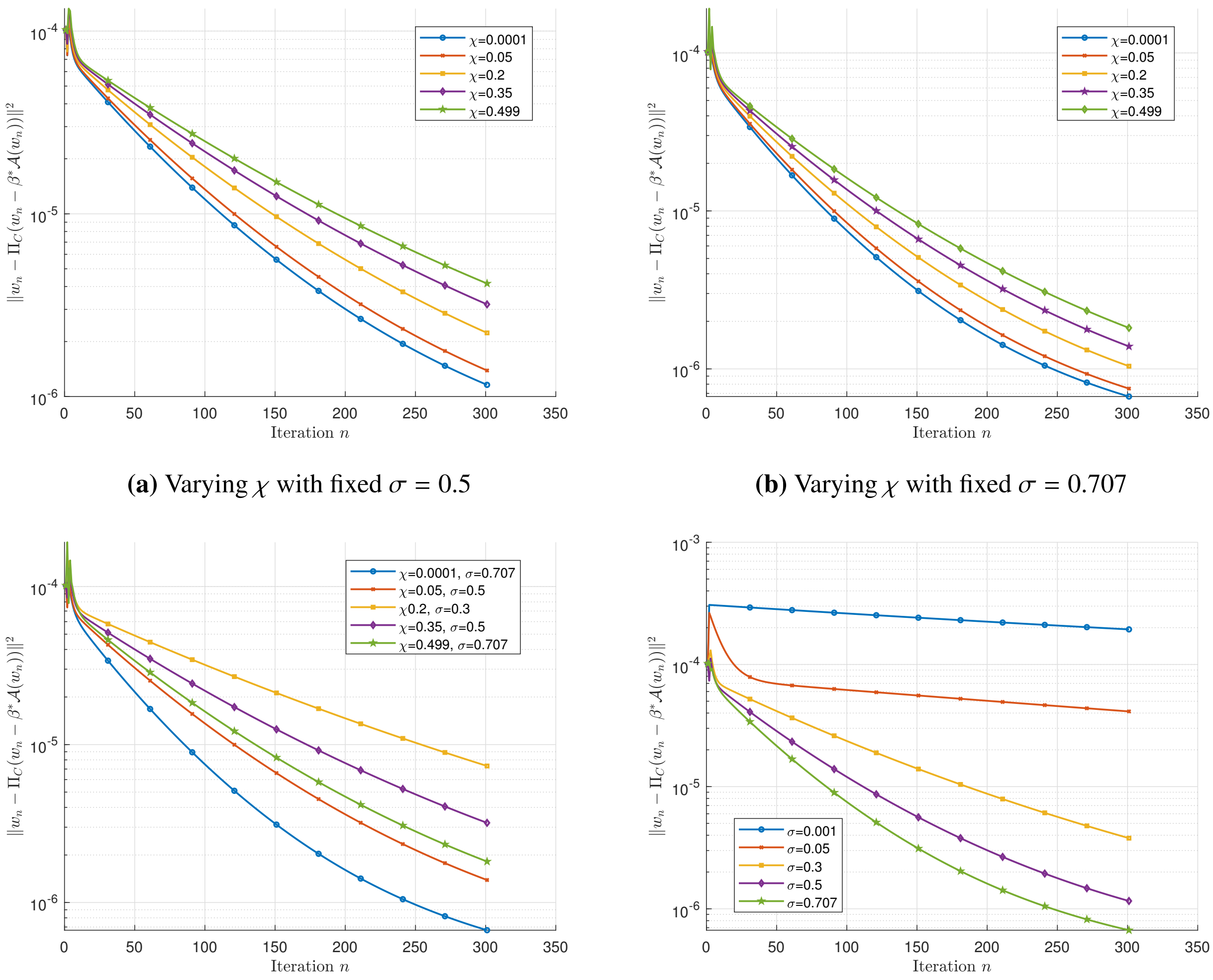

(a) Varying χ with fixed $\sigma = 0.5$

(b) Varying χ with fixed $\sigma = 0.707$

(c) Simultaneous variation of χ and σ

(d) Varying σ with fixed $\chi = 10^{-4}$

Figure 6. Convergence result of Algorithm 1 based on Example 5.1.

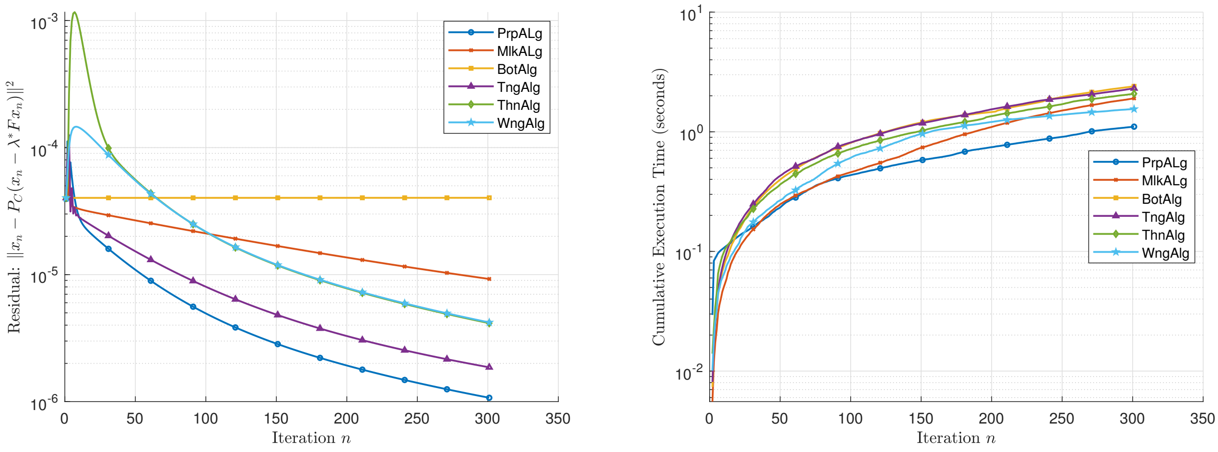

(a) Residual vs. Iteration **(b)** Cumulative Time vs. Iteration

Figure 7. Convergence results based on Example 5.1 with $m = 40$ and $l = 15$.

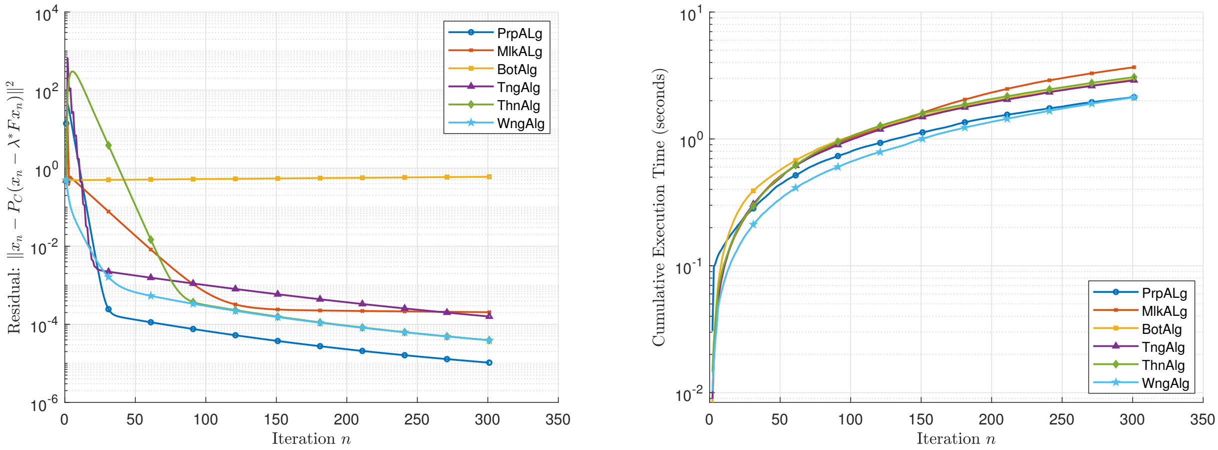

(a) Residual vs. Iteration **(b)** Cumulative Time vs. Iteration

Figure 8. Convergence results based on Example 5.1 with $m = 70$ and $l = 30$.

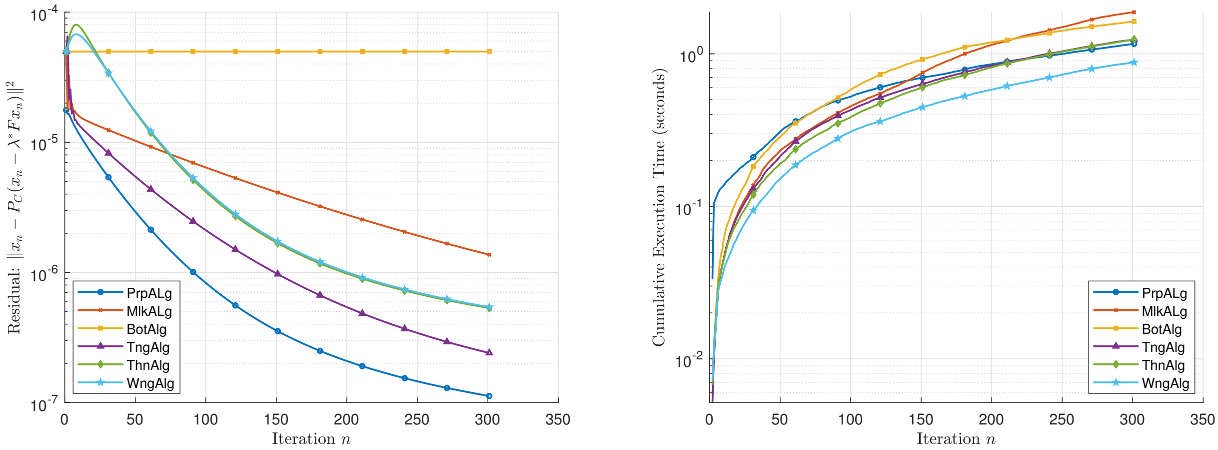

(a) Residual vs. Iteration
(b) Cumulative Time vs. Iteration

Figure 9. Convergence results based on Example 5.1 with $m = 30$ and $l = 25$.

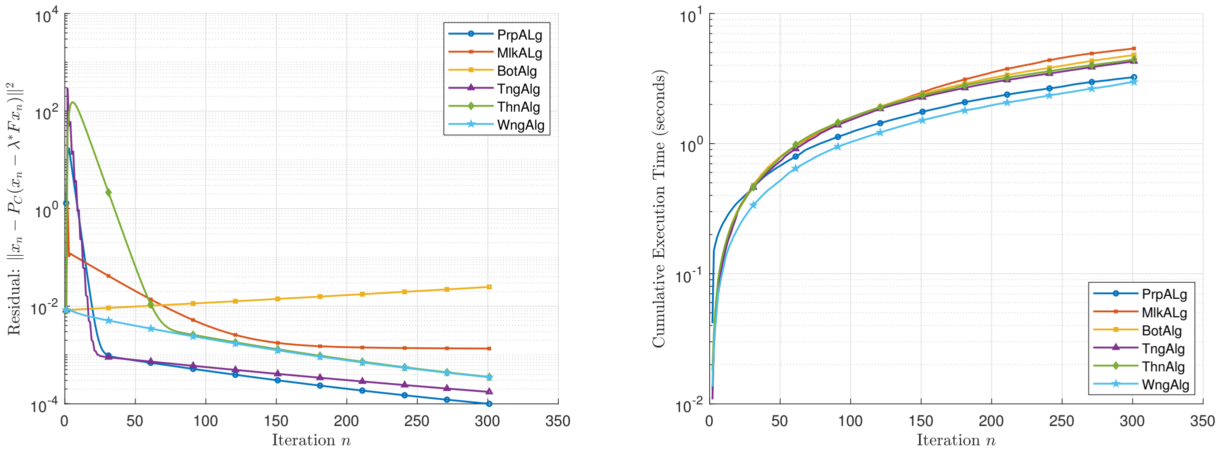

(a) Residual vs. Iteration
(b) Cumulative Time vs. Iteration

Figure 10. Convergence results based on Example 5.1 with $m = 100$ and $l = 40$.

6. Concluding remarks

This paper proposed an adaptive algorithm for approximating solutions to VIPs, with a particular focus on its application to blood supply chain networks. The proposed method, based on convex combination techniques, is designed to handle pseudo-monotone operators, providing an efficient approach even when the underlying operators are not monotone. The algorithm requires only a single metric projection per iteration and exhibits an adaptive step-size criterion.

The theoretical analysis establishes the linear convergence of the algorithm and showcases its applicability to real-world problems, particularly in healthcare systems for optimizing blood supply chains. Through numerical experiments, we have shown that the proposed method outperforms recently established algorithms in terms of convergence efficiency, making it a promising tool for large-scale network optimization problems.

Furthermore, the results of the study confirm that the proposed algorithm can provide scalable and adaptable solutions for complex network optimization problems, offering significant advantages in terms of computational efficiency and practical applicability. The ability of the algorithm to ensure the efficient management of blood supply networks is a crucial contribution to improving decision-making processes in healthcare logistics.

This work opens several avenues for future research. One promising direction involves extending the algorithm to handle more complex, dynamic systems, such as multi-period supply chain optimization or problems involving uncertainty and stochastic behavior. Additionally, applying the method to other critical logistics and supply chain networks, including pharmaceuticals and food distribution, would further demonstrate its versatility. Finally, exploring alternative step-size update strategies and enhancing the scalability of the method for even larger-scale applications will be important for broadening its impact in both theoretical and practical optimization frameworks.

Following the results obtained in Figures 3–5 and Tables 2–4, it is evident that Algorithm 1 performs reasonably and comparatively well, demonstrating promise in the context of blood supply chain networks among other problems. Notably, the compared algorithms are recognized as the best performers in this type of supply chain network, as recorded in [59, 69]. Furthermore, the results clearly show that the expected demand values remained within the acceptable uniform ranges, even before 500 iterations. Therefore, the proposed algorithm not only works effectively for cases involving pseudo-monotone operators that are not necessarily monotone, but it also appears to be competitive and promising, even among algorithms for the monotone class of operators.

Author contributions

Ghaziyah Alsahli: Conceptualization, writing – original draft, validation, methodology, conceptualization, project administration, formal analysis; Sani Salisu: Writing – original draft, review & editing, supervision, methodology, investigation; Nura Alotaibi: Writing – review & editing, validation, funding acquisition. All authors have read and approved the final version of the manuscript for publication.

Use of AI tools declaration

The authors declare they have not used Artificial Intelligence (AI) tools in the creation of this article.

Acknowledgments

This work was funded by the Deanship of Graduate Studies and Scientific Research at Jouf University under grant No. (DGSSR-2025-02-01481).

Conflict of interest

The authors declare they have no conflict of interest.

References

1. J. L. Lions, G. Stampacchia, Variational inequalities, *Commun. Pur. Appl. Math.*, **20** (1967), 493–519. https://doi.org/10.1002/cpa.3160200302
2. T. O. Alakoya, L. O. Jolaoso, O. T. Mewomo, Modified inertial subgradient extragradient method with self adaptive stepsize for solving monotone variational inequality and fixed point problems, *Optimization*, **70** (2021), 545–574. https://doi.org/10.1080/02331934.2020.1723586
3. J. Abubakar, P. Kumam, A. I. Garba, A. H. Ibrahim, W. Jirakitpuwapat, Hybrid iterative scheme for variational inequality problem involving pseudo-monotone operator with application in signal recovery, *B. Iran. Math. Soc.*, **48** (2022), 2995–3017. https://doi.org/10.1007/s41980-022-00678-z
4. J. T. Oden, N. Kikuchi, Theory of variational inequalities with applications to problems of flow through porous media, *Int. J. Eng. Sci.*, **18** (1980), 1173–1284. https://doi.org/10.1016/0020-7225(80)90111-1
5. D. Kinderlehrer, G. Stampacchia, *An introduction to variational inequalities and their applications*, vol. 31 of Classics in Applied Mathematics, Society for Industrial and Applied Mathematics (SIAM), Philadelphia, PA, 2000. https://doi.org/10.1137/1.9780898719451
6. F. Facchinei, J. S. Pang, *Finite-dimensional variational inequalities and complementarity problems. Vol. II*, Springer Series in Operations Research, Springer-Verlag, New York, 2003.
7. J. P. Aubin, I. Ekeland, *Applied nonlinear analysis*, Pure and Applied Mathematics (New York), John Wiley & Sons, Inc., New York, 1984.
8. C. Baiocchi, A. Capelo, *Variational and quasivariational inequalities*, A Wiley-Interscience Publication, John Wiley & Sons, Inc., New York, 1984.
9. G. Fichera, Sul problema elastostatico di Signorini con ambigue condizioni al contorno, *Atti Accad. Naz. Lincei Rend. Cl. Sci. Fis. Mat. Nat. (8)*, **34** (1963), 138–142.
10. R. Glowinski, J. L. Lions, R. Trémolières, *Numerical analysis of variational inequalities*, vol. 8 of Studies in Mathematics and its Applications, North-Holland Publishing Co., Amsterdam-New York, 1981.
11. E. N. Khobotov, A modification of the extragradient method for solving variational inequalities and certain optimization problems, *USSR Comput. Math. Math. Phys.*, **27** (1987), 120–127. https://doi.org/10.1016/0041-5553(87)90058-9
12. D. Kinderlehrer, G. Stampacchia, *An introduction to variational inequalities and their applications*, vol. 88 of Pure and Applied Mathematics, Academic Press, Inc. Harcourt Brace Jovanovich, Publishers, New York-London, 1980.
13. P. Marcotte, Application of khobotov's algorithm to variational inequalities and network equilibrium problems, *INFOR: Inform. Syst. Oper. Res.*, **29** (1991), 258–270. https://doi.org/10.1080/03155986.1991.11732174
14. G. Stampacchia, *Variational inequalities*, In: Theory and Applications of Monotone Operators, Proc. NATO Advanced Study Inst., Venice, 1968.
15. K. J. Arrow, L. Hurwicz, H. Uzawa, *Studies in linear and non-linear programming*, vol. II of Stanford Mathematical Studies in the Social Sciences, Stanford University Press, Stanford, CA, 1958.

16. B. T. Poljak, Gradient methods for minimizing functionals, *Ž. Vyčisl. Mat i Mat. Fiz.*, **3** (1963), 643–653.
17. V. F. Dem'janov, A. B. Pevnyi, Numerical methods for finding saddle points, *Ž. Vyčisl. Mat i Mat. Fiz.*, **12** (1972), 1094–1127.
18. G. M. Korpelevič, An extragradient method for finding saddle points and for other problems, *Ekon. Mat. Meto.*, **12** (1976), 747–756.
19. L. D. Popov, A modification of the Arrow-Hurwitz method of search for saddle points, *Mat. Zametki*, **28** (1980), 777–784.
20. Y. Censor, A. Gibali, S. Reich, The subgradient extragradient method for solving variational inequalities in Hilbert space, *J. Optim. Theory Appl.*, **148** (2011), 318–335. https://doi.org/10.1007/s10957-010-9757-3
21. Y. Censor, A. Gibali, S. Reich, Strong convergence of subgradient extragradient methods for the variational inequality problem in Hilbert space, *Optim. Method. Softw.*, **26** (2011), 827–845. https://doi.org/10.1080/10556788.2010.551536
22. B. He, A class of projection and contraction methods for monotone variational inequalities, *Appl. Math. Optim.*, **35** (1997), 69–76. https://doi.org/10.1007/s002459900037
23. Y. Malitsky, Projected reflected gradient methods for monotone variational inequalities, *SIAM J. Optim.*, **25** (2015), 502–520. https://doi.org/10.1137/14097238X
24. Y. Malitsky, M. K. Tam, A forward-backward splitting method for monotone inclusions without cocoercivity, *SIAM J. Optim.*, **30** (2020), 1451–1472. https://doi.org/10.1137/18M1207260
25. Y. Malitsky, Golden ratio algorithms for variational inequalities, *Math. Program.*, **184** (2020), 383–410. https://doi.org/10.1007/s10107-019-01416-w
26. Y. V. Malitsky, V. V. Semenov, An extragradient algorithm for monotone variational inequalities, *Cybern. Syst. Anal.*, **50** (2014), 271–277. https://doi.org/10.1007/s10559-014-9614-8
27. Y. Malitsky, Proximal extrapolated gradient methods for variational inequalities, *Optim. Method. Softw.*, **33** (2018), 140–164. https://doi.org/10.1080/10556788.2017.1300899
28. Y. Nesterov, Dual extrapolation and its applications to solving variational inequalities and related problems, *Math. Program.*, **109** (2007), 319–344. https://doi.org/10.1007/s10107-006-0034-z
29. P. Tseng, A modified forward-backward splitting method for maximal monotone mappings, *SIAM J. Control Optim.*, **38** (2000), 431–446. https://doi.org/10.1137/S0363012998338806
30. J. Yang, H. Liu, A modified projected gradient method for monotone variational inequalities, *J. Optim. Theory Appl.*, **179** (2018), 197–211. https://doi.org/10.1007/s10957-018-1351-0
31. D. Van Hieu, Y. J. Cho, P. K. Quy, N. H. Ha, An effective iterative projection method for variational inequalities in Hilbert spaces, *Soft Comput.*, **26** (2022), 10207–10221.
32. A. I. Garba, J. Abubakar, S. A. Sidi, An inertial projection and contraction scheme for monotone variational inequality problems, *Thai J. Math.*, **19** (2021), 1112–1133.
33. O. S. Iyiola, Y. Shehu, A fully adaptive method for variational inequalities with quasi-monotonicity, *Appl. Numer. Math.*, **194** (2023), 18–43. https://doi.org/10.1016/j.apnum.2023.08.005
34. K. Khammahawong, S. Salisu, Modified Halpern and viscosity methods for hierarchical variational inequalities on Hadamard manifolds, *Comput. Appl. Math.*, **43** (2024). https://doi.org/10.1007/s40314-023-02503-7

35. P. Sumalai, J. Abubakar, P. Kumam, S. Salisu, A unified scheme for solving split inclusions with applications, *Math. Method. Appl. Sci.*, **46** (2023), 14622–14639. https://doi.org/10.1002/mma.9338

36. A. Buakird, N. Nimana, N. Petrot, P. Promsinchai, A Halpern's mean subgradient extragradient method for solving variational inequalities, *Nonlin. Convex Anal. Optim.*, **1** (2022), 177–191.

37. P. Thammasiri, K. Ungchittrakool, Accelerated hybrid Mann-type algorithm for fixed point and variational inequality problems, *Nonlin. Convex Anal. Optim.*, **1** (2022), 97–111.

38. N. Pakdeerat, K. Sitthithakerngkiet, Approximatiing methods for monotone inclusion and two variational inequality problems, *Bangmod Int. J. Math. Comput. Sci.*, **6** (2020), 71–89.

39. S. Salisu, S. Sriwongsa, P. Kumam, Golden ratio method for solving monotone variational inequality problems in Hadamard spaces, *Math. Method. Appl. Sci.*, **47** (2024), 10101–10116. https://doi.org/10.1002/mma.10112

40. J. Abubakar, P. Chaipunya, P. Kumam, S. Salisu, A generalized scheme for split inclusion problem with conjugate like direction, *Math. Method. Oper. Res.*, **101** (2025), 51–71.

41. S. Salisu, S. Sriwongsa, P. Kumam, *Extragradient method for monotone variational inequality in CAT (0) spaces*, In: International Conference on Numerical Computations: Theory and Algorithms, Springer, 2023, 134–148.

42. R. I. Boţ, E. R. Csetnek, P. T. Vuong, The forward-backward-forward method from continuous and discrete perspective for pseudo-monotone variational inequalities in Hilbert spaces, *Eur. J. Oper. Res.*, **287** (2020), 49–60. https://doi.org/10.1016/j.ejor.2020.04.035

43. R. I. Boţ, M. Sedlmayer, P. T. Vuong, A relaxed inertial forward-backward-forward algorithm for solving monotone inclusions with application to GANs, *J. Mach. Learn. Res.*, **24** (2023), 1–37.

44. A. Gibali, D. V. Thong, Tseng type methods for solving inclusion problems and its applications, *Calcolo*, **55** (2018). https://doi.org/10.1007/s10092-018-0292-1

45. S. Y. Matsushita, Alternated inertial forward-backward-forward splitting algorithm, *Numer. Algebr. Control*, **14** (2024), 404–420. https://doi.org/10.3934/naco.2022035

46. A. Padcharoen, D. Kitkuan, W. Kumam, P. Kumam, Tseng methods with inertial for solving inclusion problems and application to image deblurring and image recovery problems, *Comput. Math. Method.*, **3** (2021). https://doi.org/10.1002/cmm4.1088

47. D. V. Thong, P. Cholamjiak, N. Pholasa, V. T. Dung, L. V. Long, A new modified forward-backward-forward algorithm for solving inclusion problems, *Comput. Appl. Math.*, **41** (2022). https://doi.org/10.1007/s40314-022-02104-w

48. D. V. Thong, P. T. Vuong, Modified Tseng's extragradient methods for solving pseudo-monotone variational inequalities, *Optimization*, **68** (2019), 2203–2222. https://doi.org/10.1080/02331934.2019.1616191

49. D. V. Thong, D. Van Hieu, Modified Tseng's extragradient algorithms for variational inequality problems, *J. Fix. Point Theory Appl.*, **20** (2018). https://doi.org/10.1007/s11784-018-0634-2

50. Z. B. Wang, Z. Y. Lei, X. Long, Z. Y. Chen, A modified Tseng splitting method with double inertial steps for solving monotone inclusion problems, *J. Sci. Comput.*, **96** (2023). https://doi.org/10.1007/s10915-023-02311-5

51. C. Zong, Y. Tang, G. Zhang, An accelerated forward-backward-half forward splitting algorithm for monotone inclusion with applications to image restoration, *Optimization*, **73** (2024), 401–428. https://doi.org/10.1080/02331934.2022.2107926
52. P. Li, H. K. Xu, S. Ke, Viscosity extragradient algorithms with double inertial extrapolation steps for quasimonotone variational inequalities and fixed point problems, *Optimization*, **74** (2025), 2217–2245. https://doi.org/10.1080/02331934.2024.2368070
53. A. E. Ofem, A. A. Mebawondu, G. C. Ugwunnadi, P. Cholamjiak, O. K. Narain, Relaxed Tseng splitting method with double inertial steps for solving monotone inclusions and fixed point problems, *Numer. Algorithms*, **96** (2024), 1465–1498. https://doi.org/10.1007/s11075-023-01674-y
54. D. V. Thong, V. T. Dung, P. K. Anh, H. V. Thang, A single projection algorithm with double inertial extrapolation steps for solving pseudomonotone variational inequalities in Hilbert space, *J. Comput. Appl. Math.*, **426** (2023). https://doi.org/10.1016/j.cam.2023.115099
55. Z. B. Wang, X. Long, Z. Y. Lei, Z. Y. Chen, New self-adaptive methods with double inertial steps for solving splitting monotone variational inclusion problems with applications, *Commun. Nonlin. Sci. Numer. Simul.*, **114** (2022). https://doi.org/10.1016/j.cnsns.2022.106656
56. A. Nagurney, A. H. Masoumi, M. Yu, Supply chain network operations management of a blood banking system with cost and risk minimization, *Comput. Manag. Sci.*, **9** (2012), 205–231. https://doi.org/10.1007/s10287-011-0133-z
57. A. Federgruen, G. Prastacos, P. H. Zipkin, An allocation and distribution model for perishable products, *Oper. Res.*, **34** (1986), 75–82.
58. J. Beliën, H. Forcé, Supply chain management of blood products: A literature review, *Eur. J. Oper. Res.*, **217** (2012), 1–16. https://doi.org/10.1016/j.ejor.2011.05.026
59. V. Semenov, S. Denysov, *Optimizing network economics problem with adaptive algorithms for variational inequalities*, In: Proceedings of the Workshop on Dynamical System Modeling and Stability Investigation (DSMSI-2023), Kyiv, Ukraine, 2023, 1–10. Available from: `https://ceur-ws.org/Vol-3687/Paper_1.pdf`.
60. R. Lotfi, G. W. Weber, E. B. Tirkolaee, Recent advances in viable and sustainable supply chain management, *Environ. Sci. Pollut. Res.*, **30** (2023), 89943–89944.
61. M. Zarreh, M. Khandan, A. Goli, A. Aazami, S. Kummer, Integrating perishables into closed-loop supply chains: A comprehensive review, *Sustainability*, **16** (2024), 6705.
62. A. Sepehri, E. B. Tirkolaee, V. Simic, S. S. Ali, Designing a reliable-sustainable supply chain network: Adaptive m-objective ε-constraint method, *Ann. Oper. Res.*, **359** (2026), 921–952. https://doi.org/10.1007/s10479-024-05961-2
63. A. Ala, A. Goli, S. Mirjalili, V. Simic, A fuzzy multi-objective optimization model for sustainable healthcare supply chain network design, *Appl. Soft Comput.*, **150** (2024), 111012.
64. P. Golinska-Dawson, B. Mrugalska, K. K. Lai, G. W. Weber, Editorial: Smart and sustainable supply chain and logistics–trends, challenges, methods and best practices, *Ann. Oper. Res.*, **324** (2023), 1–11. https://doi.org/10.1007/s10479-023-05304-7
65. S. Khalilpourazari, H. H. Doulabi, A flexible robust model for blood supply chain network design problem, *Ann. Oper. Res.*, **328** (2023), 701–726. https://doi.org/10.1007/s10479-022-04673-9

66. S. Khalilpourazari, A. A. Khamseh, Bi-objective emergency blood supply chain network design in earthquake considering earthquake magnitude: A comprehensive study with real world application, *Ann. Oper. Res.*, **283** (2019), 355–393. https://doi.org/10.1007/s10479-017-2588-y
67. M. Fazli-Khalaf, S. Khalilpourazari, M. Mohammadi, Mixed robust possibilistic flexible chance constraint optimization model for emergency blood supply chain network design, *Ann. Oper. Res.*, **283** (2019), 1079–1109. https://doi.org/10.1007/s10479-017-2729-3
68. S. Khalilpourazari, S. Soltanzadeh, G. W. Weber, S. K. Roy, Designing an efficient blood supply chain network in crisis: neural learning, optimization and case study, *Ann. Oper. Res.*, **289** (2020), 123–152. https://doi.org/10.1007/s10479-019-03437-2
69. S. Salisu, P. Kumam, K. Sitthithakerngkiet, Optimization of blood supply network through a perturbed forward-backward method, *J. Ind. Manag. Optim.*, **21** (2025), 3691–3720. https://doi.org/10.3934/jimo.2025028
70. L. Zhao, S. Dafermos, General economic equilibrium and variational inequalities, *Oper. Res. Lett.*, **10** (1991), 369–376. https://doi.org/10.1016/0167-6377(91)90037-P
71. A. Z. Dragicevic, Pseudomonotone variational inequality in action: Case of the French dairy industrial network dynamics, *J. Ind. Manag. Optim.*, **19** (2023), 8657–8690. https://doi.org/10.3934/jimo.2023056
72. H. H. Bauschke, P. L. Combettes, *Convex analysis and monotone operator theory in Hilbert spaces*, CMS Books in Mathematics/Ouvrages de Mathématiques de la SMC, Springer, New York, 2011. https://doi.org/10.1007/978-1-4419-9467-7
73. Z. A. Opial, Weak convergence of the sequence of successive approximations for nonexpansive mappings, *Bull. Amer. Math. Soc.*, **73** (1967), 591–597. https://doi.org/10.1090/S0002-9904-1967-11761-0
74. R. W. Cottle, J. C. Yao, Pseudo-monotone complementarity problems in Hilbert space, *J. Optim. Theory Appl.*, **75** (1992), 281–295. https://doi.org/10.1007/BF00941468
75. J. Dong, D. Zhang, A. Nagurney, A supply chain network equilibrium model with random demands, *Eur. J. Oper. Res.*, **156** (2004), 194–212. https://doi.org/10.1016/S0377-2217(03)00023-7
76. A. Nagurney, J. Cruz, J. Dong, D. Zhang, Supply chain networks, electronic commerce, and supply side and demand side risk, *Eur. J. Oper. Res.*, **164** (2005), 120–142.
77. B. Tongnoi, A modified Tseng's algorithm with extrapolation from the past for pseudo-monotone variational inequalities, *Taiwan. J. Math.*, **28** (2024), 187–210. https://doi.org/10.11650/tjm/230906